The Specialist Committee on Powering Performance Prediction

Final Report and Recommendations to the 24th ITTC

1. INTRODUCTION

1.1 Membership

The 23rd ITTC appointed the Specialist Committee on Powering Performance Prediction with the following Membership

- Prof. Neil Bose (Chairman).
  Memorial University of Newfoundland, Canada.
- Dr. Mustafa Insel (Secretary).
  Istanbul Technical University, Turkey.
- Ing. Richard Anzböck.
  Vienna Model Basin, Austria.
- Mr. Seung-Myun Hwangbo.
  Samsung Heavy Industries, Korea.
- Mr. Friedrich Mewis.
  Hamburg Ship Model Basin, Germany.
- Dr. Sverre Steen.
  Norwegian Marine Technology Research Institute, Norway.
- Dr. Naoji Toki.
  Mitsubishi Heavy Industries, Japan.
- Dr. De-Xiang Zhu.
  China Ship Scientific Research Center, Shanghai Branch, China.

1.2 Meetings

At the first meeting Mustafa Insel was elected Secretary of the Committee. Meetings were held as follows:

- Istanbul Technical University, Turkey, January 2003.
- Vienna Model Basin, Austria, October 2003.
- China Ship Scientific Research Centre, Shanghai Branch, March 2004.
- Memorial University of Newfoundland, Canada, November 2004.

2. TASKS SET FROM THE 23rd ITTC

Task 1: Review and update the Speed/ Powering Trials Procedures 7.5-04-01.1 – 7.5-04-01.6 and include analysis and take due account of the ISO Standard Guidelines

Task 2: Examine new extrapolation techniques for powering prediction, including numerical methods such as the use of RANS codes. Develop corresponding correlation factors, if necessary

Task 3: Develop the uncertainty analysis of extrapolation methods as follows:
- Accumulate trial results analysed by using several extrapolation methods
- Complete the evaluation of the uncertainty analysis for power prediction by making use of uncertainty analysis for model scale self-propulsion and open water tests
- Perform validation of extrapolation methods for power prediction by comparing with speed trial data and full-scale tests, including uncertainty analysis

Task 4: In co-operation with the Seakeeping Committee review the state of art and recommend a standard procedure for predicting powering margins.

3.   FOREWORD

The Committee tasks included the review of the existing speed/powering trials procedures; an extensive program on evaluation of model to ship extrapolation methods; and the recommendation of a procedure for predicting powering margins.

The trials procedures were reviewed and the intention of the Committee has been to produce a new simplified procedure for the conduct of trials by amalgamating the six existing procedures. Additionally a new procedure for the analysis of speed/powering trials was formulated.

On extrapolation methods, first the Committee made a review of existing methods in use. These were found to include many methods based around the inclusion of results from resistance, propeller open water and self-propulsion tests (all similar but with many variations of details such as different friction lines; inclusion of a form factor or not; etc.); a small number of extrapolations based only on the results from load varied self-propulsion tests; the possibility of using results from quasi-steady self-propulsion tests; and the possibility of doing extrapolations using RANS numerical simulations. For the latter, a survey was made of model tanks to assess the level of usage and it was found that there is currently no commercial usage of RANS methods for model/ship extrapolation for powering prediction.

To assess the uncertainty in extrapolation methods and to work towards the development of reliable correlation factors associated with different methods, the Committee first assembled a database of ship model experimental results and corresponding full scale trials data.

This included both individual vessels of different types and series of several ships to the same design. In addition, for one series of 13 vessels, from the Vienna Model Basin, a model was constructed and a wide program of repeat tests was done to ascertain uncertainty levels and to provide data from load varied tests.

The Committee adopted Monte Carlo methods instead of conventional uncertainty analysis recommended by the 22nd and 23rd ITTC due to increasing complexity of the data reduction equations. Uncertainty analysis for extrapolation methods was performed for both the ITTC 1978 method and the method based on self propulsion tests alone.   The results of these are described in the report.

Full scale speed/powering trials suffers from both measurement uncertainties and uncertainties due to corrections for environmental conditions such as wind, waves, shallow water etc. Uncertainty analysis based on trials of a series of 12 vessels was performed by use of Monte Carlo methods and results are presented in the report.

Due to the size of the task and time restrictions, the Committee was not able to complete the work on analysis of extrapolation methods, development of correlation factors and uncertainty analysis, but has made considerable inroads into the work. The database was collected to use as a resource to be able to develop correlation factors relevant to different extrapolation methods as well in the small variations in the methods. The results from the model tests were also obtained to assist with this analysis.   Uncertainty analysis may be applied to the vessels in the data set to investigate the agreement between extrapolated results and sea trials.   Further assessment of uncertainty levels between different extrapolation methods would be valuable.   Also, the database could be extended to include a broader range of ship types.

The issue of powering margins was reviewed.   Few reliable methods exist for accu-

rately predicting powering margins. However, the Committee prepared a draft procedure for the estimation of powering margins which we strongly suggest is reviewed by a Committee of the 25th ITTC.

4.   PREPARATION, CONDUCT AND ANALYSIS OF SPEED/POWERING TRIALS

The previous Procedures 7.5-04-01.1 to 7.5-04-01.6 dealing with how sea trials should be performed were amalgamated into one Procedure, which was called "Procedure for the Preparation and Conduct of Speed/Power Trials". These previous procedures, although useful, did not reflect common practice on sea trials and were not straightforward to follow for sea trials on conventional ships. The new shortened procedure is applicable to speed power trials performed on conventional commercial ships of displacement type; the recommendations might not be sufficient for trials with navy ships or with planning craft.

With respect to the Committee's task to take account of the ISO Standard Guidelines, the "Trial Conditions", as they now are proposed in the procedure match well with the limits for wind and sea states given in the ISO-Standard 19019.

Concerning environmental influences on the performance of sea trials, speed runs should only be performed against and with the waves. The correction methods existing so far account for the influences of waves only for these two conditions; in the case when waves do not come from the bow or the stern the correction methods are not sufficiently reliable and the effects of steering and drift on the ship's performance might be underestimated.

Sheltered areas provide the comfort of protection from waves, but normally in these areas shallow water effects have to be considered. When choosing a trials site, the advantage of an accepted and simple correction for shallow water effects may be preferred against doubtful corrections for the effects of waves, steering and drift.

Following the tasks given to the Committee a "Procedure for the Analysis of Speed /Power Trial Data" was proposed to the 24th ITTC; and the procedure follows a methodology similar to the one recommended by ISO 15016.

The proposed method to analyse speed/power trial data is based on thrust identity and the knowledge of the thrust deduction fraction, the wake fraction, the relative-rotative efficiency and the propeller open water characteristics of the full scale propeller are required. If this information is not known from model tests it can be derived from reliable statistics. The propeller open water data might be obtained from the propeller manufacturer.

Ideally, the wind resistance coefficients of the ship should be obtained from model tests. In most cases model tests are not available and reliable statistical values can be used.

For the correction of wave effects the knowledge of the response functions of the ship in question in head- and following seas is required. In many cases they are not available. Reliable methods to correct for the effect of waves without having carried out model tests are not yet available.

Methods to correct for roughness effects on propellers and for roughness and fouling on a ship's hull are of doubtful accuracy to date.

It is therefore recommended to perform sea trials in such a way that only corrections which are state-of-the-art and have been already proven reliable are applied to the measured trial data. Corrections should concentrate on essential environmental conditions such as wind, waves and shallow water; correction methods, which might lead to unreliable results, should be avoided.

5. REVIEW OF EXTRAPOLATION METHODS

5.1 RANS Methods

For examination of the state-of-the-art in using new extrapolation techniques for powering prediction, including numerical methods, the Committee decided to send a questionnaire to all Member Organizations. The first run in February 2003 resulted in 21 answers from 110 organizations, a second run in February 2004 resulted in altogether 35 answers from Member Organizations (32% of 110). The summary of the results is given in the following Section.

In Table 5.1 the answers to the first three questions are summarized.

- Question 1: Do you use viscous flow codes for flow calculations?
- Question 2: Do you use free surface codes?
- Question 3: Do you have in development or in use a new extrapolation technique including numerical methods such as the use of RANS-codes?

Table 5.1- Results of questioning to the use of RANS – codes, altogether 35 participants.

Question No.	1	2	3
Question contents	use of RANS codes	free surface	extrapolation technique
Organizations	35	30	35
Yes	30	25	12
% of all	86	71	34

The summary to answers of the following four questions is given in Table 5.2 below.
- Question 4: Please define the area in which the code is used for model and full scale.
- Question 5: Have you developed corresponding correlation factors?
- Question 6: Have you performed an uncertainty analysis for this technique?
- Question 7: Do you believe that using numerical methods can or will lead to better extrapolation methods?

The results of the questioning show that 10 out of 35 (29%) organizations are using RANS-codes for calculating the ships resistance and 8 of 35 (23%) for calculating the wake field. For powering calculations RANS-codes are not in use up till now.

Correlation factors are in use at 5 of 35 (14%) of the organizations answering. Correlation factors are used in R&D projects mainly. It was mentioned that correlation factors should be developed during the next few years.

Most of the answering organizations do expect that numerical methods can or will lead to better extrapolation methods. The highest expectation is for resistance of appendages (80%) and wake field (77%).

5.2 Review of Extrapolation Methods in Use

The Committee collected a description of the standard ship powering extrapolation methods in use at each of the organizations represented on the Committee. The results were compiled in Table 5.3, on the following page.

Table 5.2- Results of questioning to the use of RANS – codes, all together 35 participants.

Question No.	4	5	6	7
Question contents	area	correlation factors	uncertainty analysis	future
Organizations	25	5	3	35
Resistance of the whole ship	10	0	2	25
Resistance of appendages	5	2	1	28
Resistance of passive propulsion devices	3	1	0	22
Wake-field	8	3	2	27
Propeller characteristics	4	2	1	23
Power of the whole ship	0	0	0	19
Others	4	1	0	8

Table 5.3- Compilation of extrapolation methods in use at the organizations represented on the Committee (Question marks indicate that the information was not available).

Organization	Form factor	Wind resistance	Bilge keels	Wake scaling	K_T, K_Q scaling	Propulsion analysis	Roughness correction	Friction line	Blockage correction	Correlation allowance
A	k=0	Calculated	Calc. Frictional resistance	Tanaka Sasajima	ITTC'78	Thrust identity		ITTC'57	?	C_A
B	k=0	Calculated	?	Tanaka Sasajima	ITTC'78	Thrust identity	ΔC_F=0.00035-Ls*2E-6	ITTC'57	?	C_P, C_N
C	Empirical formula	Calculated	Calc. Frictional resistance	Tanaka Sasajima	No	Thrust identity		ITTC'57	Scott's formula	C_A
D	k=0	Calculated	?	Tanaka Sasajima	ITTC'78	Thrust identity	No, included in C_A	ITTC'57	No	$C_A=\Delta C_F$+statistics
E	Fine ships: k=0 Full ships: k=0	Calculated	Tests are performed with bilge keels which are considered as part of the hull.	either empirical	Run POW tests at two revs, one for prop. Test and one for prediction	Thrust identity	own empirical relation	Fine ships: Prandtl-Schlicting Full ships: Hughes	No	Wake and roughness allowance
F	k=0	Calculated	Estimated, based on experience data	Yasaki	Lerbs-Meyne (1972)	Thrust identity	Included in C_A	ITTC'57	Yes	C_A= f(L_{PP},C_B)
G	Fine ships: k=0 Full ships: k=0	Fine ships: incl. in C_R Full ships: Calculated	?	Tanaka Sasajima	No?	Thrust identity	ITTC'78 (only full ships)	ITTC'57	?	C_A
H	k found by Prohaska's method	Calculated	Wetted surface of bilge keels added for full scale	Tanaka Sasajima	ITTC'78	Thrust identity	ITTC'78	ITTC'57	No	C_P, C_N (ITTC'78)

It was found that all organizations use traditional extrapolation methods along the lines of the ITTC 1978 method, but with a varying level of customisations. All use thrust identity in the propulsion analysis, and all except one use the ITTC 1957 friction line. All institutions, with one exception, separate the air resistance by use of simple empirical formulae. Tanaka Sasajima (e.g. Carlton 1994) is used for wake scaling by all except two. Only one institution determined form factor by Prohaska's method. Most institutions use k=0 (two-dimensional extrapolation). Only one institution applies their correlation correction on revolutions and power; all the others apply the correlation correction on the resistance. The two items with the largest variation between institutions were roughness correction and scaling of propeller characteristics (open water curve, K_T, K_Q scaling). This probably shows that these two items need more (published) research in order to reach a level of knowledge and confidence that is accepted by most institutions. A review on the effects of roughness and fouling has been reported in a later Section.

5.3 Review of Extrapolation Techniques Using Self Propulsion Test Results Only

Several extrapolation techniques for full scale ship powering prediction from model experiments are based on the results from load varying self-propulsion tests only (i.e. they do not use a combination of resistance, propeller open water and self propulsion tests). Many towing tanks have such procedures incorporated into their guidelines of standard practice and may or may not use them on a regular basis for ship powering prediction. At least one major model basin does powering predictions using this approach for reliability and cost reasons (fewer tests mean lower model testing costs), although it will provide extrapolated

power to clients using the methods that they request (often using the ITTC 1978 method).

Early documented approaches to such techniques have been described by Schmiechen (e.g. Schmiechen 1991) and Kracht (1991). Schmiechen's "Rational Theory" was further elucidated by the 22nd ITTC Specialist Committee on Unconventional Propulsors (Bose et al. 1999). However, more straightforwardly and incorporating much more easily applied procedures, have been the methods described in detail by Holtrop (2001) and Molloy/Bose (Molloy 2001; Molloy and Bose 2001; Bose and Molloy 2001).

Briefly the approach consists of the following steps:

1. Carry out load varying self-propulsion test.
2. Obtain the thrust deduction fraction directly from the load varying test data.
3. Calculate the ship self propulsion point.
4. Optional: Obtain the form factor.
5. Extrapolate full scale thrust at the ship self propulsion point.
6. Or: Obtain the effective model resistance (towing force at zero propeller thrust), extrapolate the resistance and obtain the full scale thrust through application of the thrust deduction fraction.
7. Estimate the wake scale effect.
8. Correct the thrust and torque coefficients for Reynolds number scale effects of the drag over the propeller blades.
9. By consideration of the required thrust relation K_T/J^2 and its intersection with the estimated full scale propeller thrust coefficient curve, obtain the advance coefficient of the full scale propeller operating point and the thrust and torque coefficients.
10. Hence obtain the revolutions, delivered power, thrust, torque, etc. of the full scale ship.

It was the intention of the Committee to do a series of extrapolations for ships where both load varying model tests and full scale trials data were available to assess variations in effective model/full scale correlation coefficients. Unfortunately, it was not possible to assemble sufficient data for more than a handful of ships to make this task meaningful. Data was available for the R-Class icebreaker (see Bose and Molloy 2001) and tests were done at the Vienna Model Basin for a family of ships.

5.4 Data From Quasi-Steady Self-Propulsion Tests

Holtrop and Hooijmans (2002) proposed a quasi-steady method of collecting data from load varied self-propulsion tests. The intention of the method is to reduce the testing time necessary in a self-propulsion test to collect substantial load varied data over a range of model speeds. They proposed the approach as especially suitable for tests on complex and hybrid propulsor arrangements, but in fact the approach can be used in any load varied self-propulsion test.

In the quasi-steady method, a gradual variation of the rotational speed of the propeller/s is imposed, while the forward speed of the ship model is kept constant. The load of the propeller/s changes continuously throughout the measurement run. The data, of forward speed, total thrust, total torque, propeller revolution speed and towing force, is collected digitally. The assumption of the quasi-steady experiments is that each instantaneous data set is representative of the corresponding steady condition: i.e. it is assumed that the rate of change of the measured parameters is small compared with the time differences incurred in the data collection process between the measurement of each channel; and that physically the rate of change in the measured parameters is relatively small between data sets such that each measured value can be considered to represent its steady value relative to the measured values of its corresponding parameters.

A regression analysis is done on the data and from this a numerical model of the propul-

sion characteristics from the test are determined. These are then used in an extrapolation process of choice (one which makes use of load varied data). The extrapolation method described in the previous Section would be an obvious choice, but the propulsive characteristics could also be used in an extrapolation process such as the ITTC 1978 approach, or its derivatives. Details of the use of data obtained in this way, in an extrapolation method using only the results from self-propulsion tests (e.g. Holtrop 2001), are described by Holtrop and Hooijmans (2002).

Holtrop and Hooijmans (2002) also explain that, strictly, the measured torque should be corrected for the inertia torque induced by the changes in the rotational speed of the propeller/s, but that in normal model tests these are quite small compared with the hydrodynamic torque.

6. MODEL TESTS-TRIALS DATABASE

A database of sea trials was established by the Committee Members. The main contribution was made by the Vienna tank for twin screw vessels and by HSVA on large container ship sea trials. 110 sea trials data were collected for 48 different ship forms. Data for both twin screw and single screw vessels were collected (55 of each). Fifty three of the ships have fixed pitch propellers

Containerships and ferries are the main ship types in the database with a population of 42 and 41 respectively as given in Fig. 6.1. Distribution of ship length is given in Fig. 6.2. Sixty five out of 110 sea trials were for 120 to 180 m long ships. Froude number at the maximum trial speed was mainly between 0.225-0.325 indicating performance in the displacement regime Fig. 6.3.

Environmental conditions are given in Figs. 6.4 and 6.5. The wave height in trial conditions ranges up to 1.5% ship length, meanwhile the water depth/ship length ratio 0.2-0.4 was used

commonly for 48 ships. Displacement in trial conditions is within 10% of contract conditions for the majority of ships in the database Fig. 6.6.
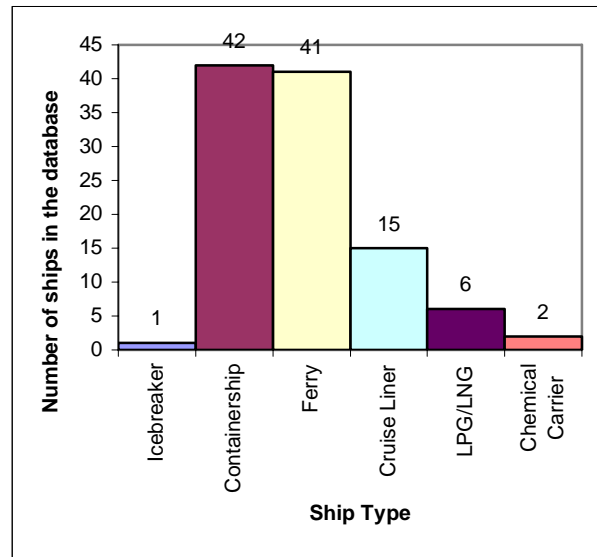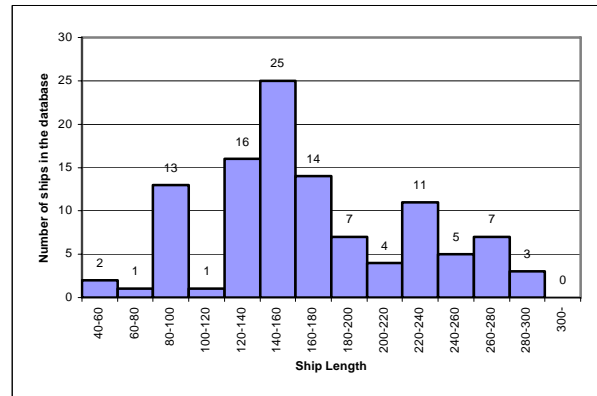

Figure 6.1- Ship types in the database.

Figure 6.2- Ship length in the database.

7. EVALUATION OF EXTRAPOLATION TECHNIQUES

7.1 Analyses of Sea-Trial Data by Use of Different Friction Lines

In one study, sea-trial data accumulated at one organization over more than 30 years were analysed by using different friction lines. The trial analysis and power estimation procedures

of the organization are very close to the ITTC 1978 method, but not exactly the same.
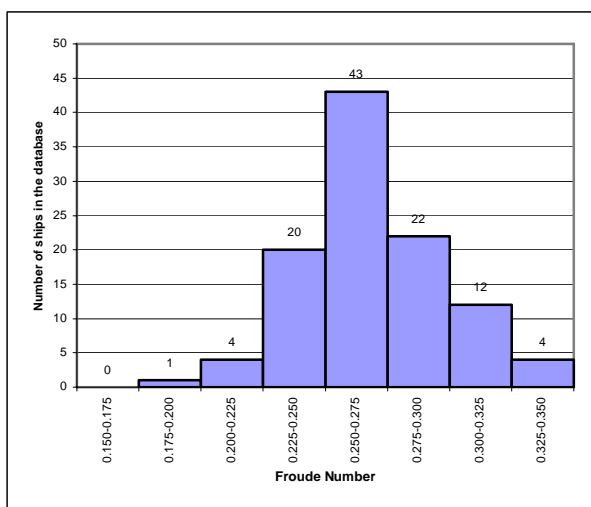

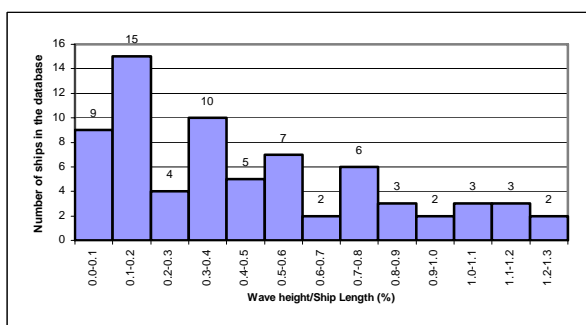Figure 6.3- Maximum Froude number of trials.

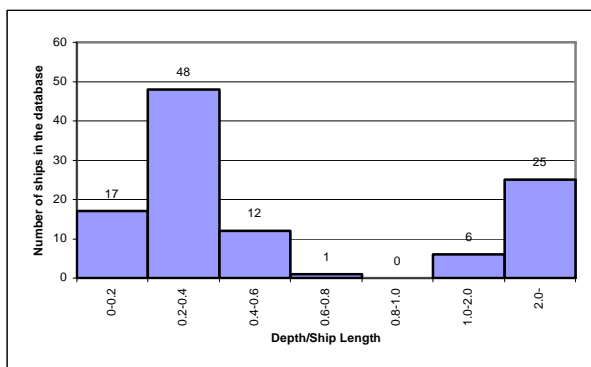Figure 6.4- Wave conditions in the trials.
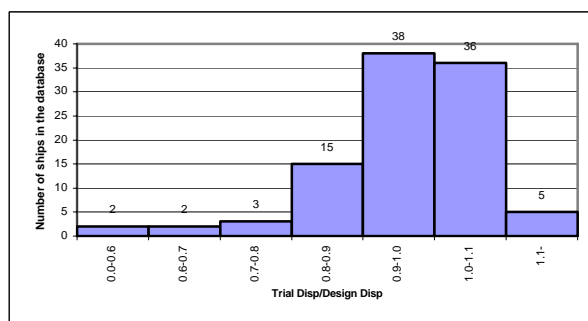

Figure 6.5- Water depth in the trials.

Figure 6.6- Trial Displacement / Design Displacement.

Two runs in opposite directions with the same level of engine output were considered as a base set of trial runs. Data measured at the trials were corrected for the effects of wind and current, and a set of values for ship speed against water, shaft horsepower and propeller revolutions were obtained from the measurements for a base set of trial runs. It is called "a data set of sea-trial". Here, more than 1,200 data sets were analysed.

Friction lines. The following friction lines were used in the analysis:

1. Hughes' basic line
$$C_f = \frac{0.066}{(\log_{10} R_n - 2.03)^2}$$

2. ITTC 1957 line
$$C_f = \frac{0.075}{(\log_{10} R_n - 2)^2}$$

3. Grigson's line

4. Katsui's line

Grigson's line and Katsui's line are obtained by the numerical integration of local friction in the boundary layer, and have no analytical forms. Grigson's line was approximated by,

$C_f f = 10^A$ where,

$A = 2.98651 - 10.8843 \cdot B + 5.15283 \cdot B^2$

   when, $2 \times 10^5 \le R_n \le 10^7$

$A = -9.57459 + 26.6084 \cdot B - 30.8285 \cdot B^2$

   $+ 10.8914 \cdot B^3$ when, $10^7 \le R_n \le 6 \times 10^9$

$B = \log_{10}(\log_{10} R_n)$

and, Katsui's line is approximated by,

$$C_f = \frac{0.0066577}{(\log_{10} R_n - 4.3762)^{0.042612 \cdot \log_{10} R_n + 0.56725}}$$

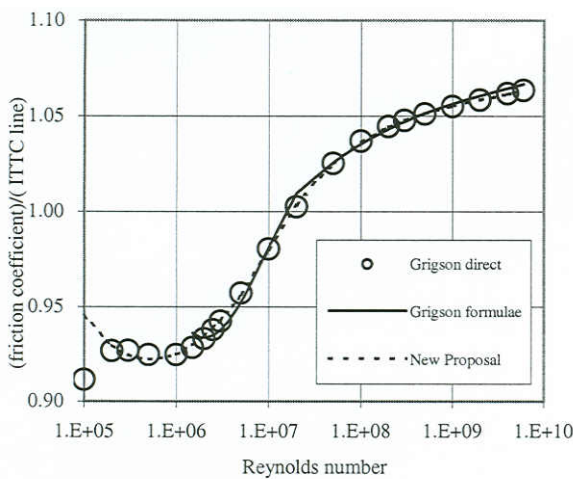The comparison between this approximation and other forms of Grigson's line is shown in Fig. 7.1.

Figure 7.1- Comparison between approximate and direct forms of Grigson's Friction Line.

Conversion of Data for Different Friction Lines. The sea trial data were accumulated by using one friction line. Those data were converted here into the ones using different friction lines, in the following way.

At first, form factor k, was converted by the following formula (on the assumption that the wave-making term can be neglected at F_n=0.1,

$(1 + k) \times C_f = (1 + k') \times C_f'$, for F_n=0.1

Here, C_f is frictional resistance coefficient calculated by the original friction line and C_f' is the one calculated by an alternative friction line.

Calculating the values of frictional resistance coefficient by two lines for the Reynolds number given by

$$R_n = \frac{v_m \times L}{\nu} = \frac{F_n \times \sqrt{g \cdot L^3}}{\nu} = \frac{0.1 \times \sqrt{g \cdot L^3}}{\nu},$$

k' was obtained by the following formula.

$$k' = (1 + k) \times \frac{C_f(R_n)}{C_f'(R_n)} - 1$$

Next, a new value of C_w was calculated for each case of trial runs. From the value of advance speed: v, Froude and Reynolds numbers were calculated by,

$$F_n = \frac{v}{\sqrt{g \times L}}, \quad R_n = \frac{F_n \times \sqrt{g \times L^3}}{\nu}$$

Because the value of total resistance coefficient remains the same

$$C_t = C_w(F_n) + (1 + k) \times C_f(R_n) \times \frac{S}{\nabla^{2/3}}$$

$$= C_w'(F_n) + (1 + k') \times C_f'(R_n) \times \frac{S}{\nabla^{2/3}},$$

the new value of wave-making resistance coefficient: C_w' was calculated by the following formula. Here, total resistance and wave-making component were non-dimensionalized by using $\nabla^{2/3}$, frictional resistance component was non-dimensionalized by using wetted surface area S.

$$C_w(F_n) = C_w(F_n r) + \{(1 + k) \times C_f(R_n)$$

$$- (1 + k') \times C_f'(R_n)\} \times \frac{S}{\nabla^{2/3}}$$

Then, the trial analysis procedure was followed by use of different friction lines.

Analysis Procedure. For the case of each friction line, after getting correlation factors, which are ΔC_f and $e_i = (1-w_m)/(1-w_s)$, linear regression formulae were established for them by use of $\log(R_n)$, displacement ratio to the fully loaded condition, engine output ratio to MCR output, etc. Using the formulae, ΔC_f and e_i were estimated for each data set, and the values of required power HP and propeller revolution N_P were estimated. Then, the values of C_{power} and C_n were calculated by the following formulae.

$$C_{power} = \frac{HP_{Measured}}{HP_{Estimated}}$$

$$C_n = \frac{N_{P,Measured}}{N_{P,Estimated}}$$

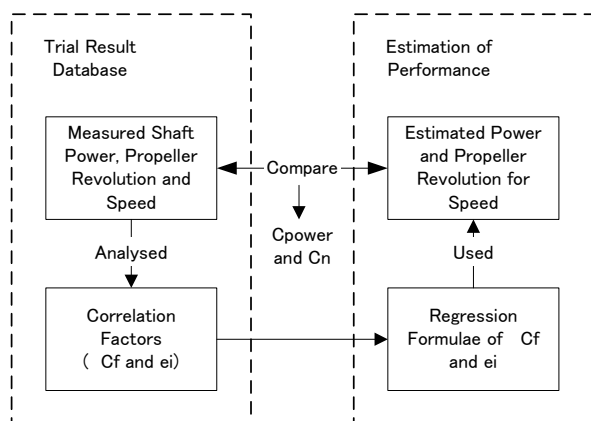The flow of the analysis is illustrated in Fig. 7.2.

Figure 7.2- Flow of the analysis.

Another series of calculations were performed by use of Townsin's formula:

$$\Delta C_f = 0.044 \cdot \left\{ \left(\frac{\kappa}{L} \right)^{1/3} - 10 \cdot R_n^{-1/3} \right\}$$
$$+ 0.000125$$

instead of the linear regression formula using $\log(R_n)$.

In the analysis, mean values of C_{power} and C_n are supposed to be very close to 1.0. Only the scatter in them is meaningful.

Results. One example of the obtained values of C_f ($C_{f,s}$) is illustrated in Fig. 7.3, where $C_{f,s}$ is calculated by the following formula.

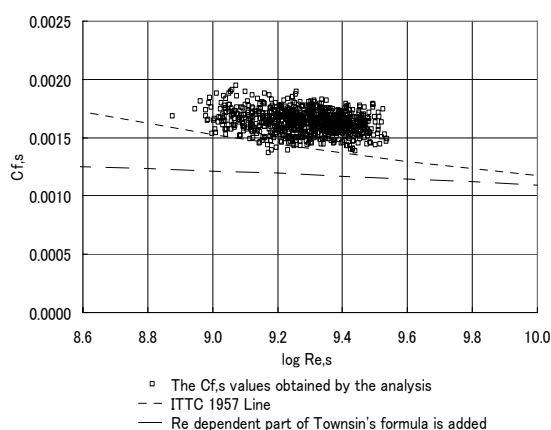$$C_{f,s} = \frac{(C_{t,s} - C_w)}{1+k} \cdot \frac{\nabla^{2/3}}{S}$$

Figure 7.3- The obtained $C_{f,s}$ values vs. log (R_e).

$C_{t,s}$ is the estimated total resistance coefficient from measured torque during sea trial, propeller characteristics and self propulsion factors. The difference between the values of $C_{f,s}$ and C_f given by the friction line is ΔC_f.

By using Townsin's formula, ΔC_f values were converted to C_A values which are defined by the following formula.

$$C_A = \Delta C_F - \Delta C_{F,Townsin} = \Delta C_F$$
$$- 0.044 \left\{ \left(\frac{\kappa}{L} \right)^{1/3} - 10 \cdot R_e^{-1/3} \right\} + 0.000125$$

Mean values, standard deviations and histograms of C_A were calculated for the cases for the given friction lines. Mean values and standard deviations are shown in Table 7.1, and the histograms are shown in Fig. 7.4.

Mean values of C_A are considered close enough to zero. It means that the Reynolds number dependent part of ΔC_f can be expressed well by Townsin's formula. However, ΔC_f and C_A values depend on not only the friction line used but also on the estimation procedure of the full-scale propeller open characteristics, which of this organization is not the same as the one in ITTC 1978 method. Therefore, further consideration is desirable.

Validity of the roughness dependent part of Townsin's formula could not be verified, because the majority of data are not accompanied with the results of hull roughness measurements.

The mean values and standard deviations of C_{power} and C_n were calculated for each case, and the mean values resulted in the values being very close to 1.0 as expected. The values of standard deviation are shown in Tables 7.2

and 7.3. There are slight differences in the results, but they can be considered negligible. Standard deviations of C_{power} and C_n remain around 5% and 1.5% for all the cases.
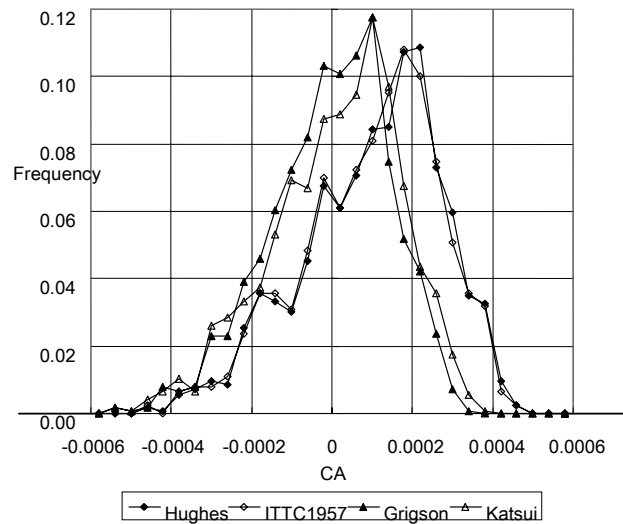

Figure 7.4- Histograms of the obtained CA values.

Table 7.1- Results of Calculations (Linear Regression of Log(R_n) is used for each case).

	Hughes	ITTC	Grigson	Katsui
Mean of C_A	0.000061	0.000056	-0.000045	-0.000030
St. Dev. of C_A	0.000172	0.000171	0.000150	0.000162

Table 7.2- Results of Calculations (Linear Regression of Log(Rn) is used for each case).

	Hughes	ITTC	Grigson	Katsui
St. Dev. of C_{power}	0.0495	0.0495	0.0480	0.0487
St. Dev. of C_n	0.0153	0.0153	0.0149	0.0151

Table 7.3- Results of Calculations (Townsin's Formula is used).

	Hughes	ITTC	Grigson	Katsui
St. Dev. of C_{power}	0.0508	0.0507	0.0486	0.0497
St. Dev. of C_n	0.0155	0.0155	0.0150	0.0152

Standard deviations are slightly but uniformly increased by use of Townsin's formula instead of the regression formulae of log(R_n). This is because the variation of ΔC_f vs. log(R_n) for the case of each friction line does not necessarily coincide exactly to the tendency given by Townsin's formula.

8. ESTIMATION OF UNCERTAINTY WITH MONTE CARLO METHODS

8.1 Conventional Uncertainty Assessment Methodology

The 22nd ITTC recommended a methodology for estimating uncertainty in measurements

and results calculated from these measurements for towing tank tests. The methodology is based on the assumption that error in a measurement is composed of bias (systematic) errors and precision (random) errors. An error is classified as precision error if it contributes to the scatter of the data, otherwise it is a bias error.

For a calculated value of variable r which is a function of various measurements, a data reduction equation can be given as:

$$r = r(X_1, X_2, X_3....X_J)$$

where,
r is the experimental result determined from J measured variables X_i. Each of the measured variables contains bias and precision errors.

Error is defined as the difference between an experimentally determined value and the true value. An estimate of the error is defined as the uncertainty which is made at some confidence level, such as 95%. This means that the true value of the quantity is expected to be within $\pm U$ interval about the experimentally determined value 95 times out of 100.

A precision limit (P) is defined as an estimator of the precision errors. A 95 % confidence estimate of P is interpreted to mean that the $\pm P$ interval about a single reading of X_i should cover the population mean 95 times out of 100.

The precision limit is estimated from the scatter in the measured values by

$$P_r = K\,S_r$$

where,
K is the coverage factor and is equal to 2 for 95% confidence interval and large sample size ($N \geq 10$) and S_r is the standard deviation of the sample of N readings of the result r.

The bias limit (B) is defined as an estimator of bias errors. A 95 % confidence estimate is

interpreted as the experimenter being 95 % confident that true value of bias error would be within $\pm B$. The bias limit of a measurement can be given by:

$$B_r^{\,2} = \sum_{i=1}^{J} \theta_i^{\,2} B_i^{\,2} + 2\sum_{i=1}^{J-1}\sum_{k=i+1}^{J} \theta_i \theta_k B_{ik}$$

where,
θ_i are sensitivity coefficients

$$\theta_i = \frac{\partial r}{\partial X_i}$$

B_i are the bias limits in X_i, and B_{ik} are the correlated bias limits in X_i and X_k.

$$B_{ik} = \sum_{\alpha=1}^{L} (B_i)_\alpha (B_k)_\alpha$$

where,
L is the number of correlated bias error sources that are common for measurement of variables X_i and X_k.

The total uncertainty limit in r is expressed as root-sum-square (RSS) of bias and precision limits.

$$U_r^{\,2} = B_r^{\,2} + P_r^{\,2}$$

Hence the procedure in the conventional uncertainty assessment methodology (Fig. 8.1) is:

a) Determine bias errors in elemental error sources
b) Combine elemental errors into measured individual variable errors by taking root-sum-square
c) Propagate bias errors in measured individual variable errors through data reduction equation
d) Perform repeat tests (minimum 10) and find standard deviation
e) Take twice the standard deviation to find precision limit (for 95% confidence)
f) Root-sum-square bias and precision errors to find total uncertainty limit

If the same elementary error sources are shared among individual measurement variables, then correlated bias errors must be taken into account. Temperature measurement error is a good example for such elemental error sources for correlated bias errors. Measurements taken from the same equipment have correlated bias errors. For example, this is the case for form factor tests at low speed for Prohaska analysis.

If data reduction equations get complicated, application of conventional uncertainty assessment methodology becomes cumbersome. For example, derivations of partial differential equations and finding correlated bias errors are almost prohibitive for ship model to ship extrapolation by the ITTC 1978 method.
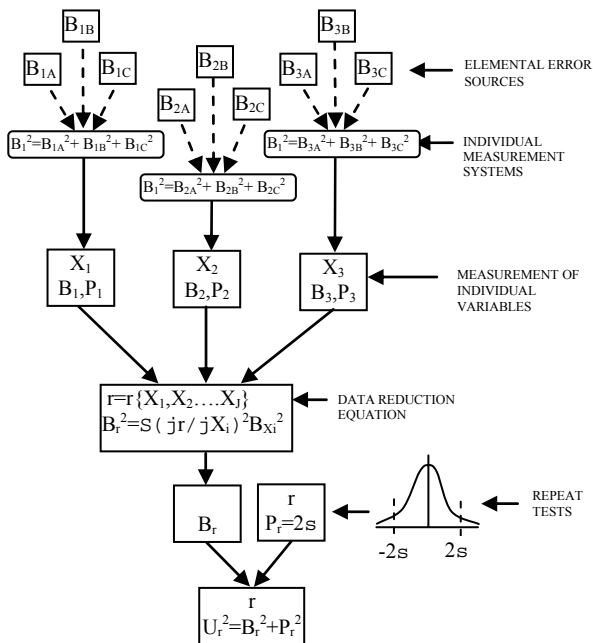
Figure 8.1- Conventional uncertainty assessment methodology.

8.2 Uncertainty Assessment Methodology by Monte Carlo Method

The Monte Carlo method can be applied into uncertainty estimation as an alternative approach to such problems. The methodology (Fig. 8.2) is based on:

a) Determine elemental bias/precision error sources and their bias/precision limits.
b) Create Gaussian (or other) error distributions of bias/precision errors by assuming a standard deviation equal to half of bias/precision error limit (for 95% confidence).
c) Create a calculation model by using data reduction equations. If an elemental bias/precision error source is shared among two or more variables, the same random value of elemental bias/precision error value is used in those variables.
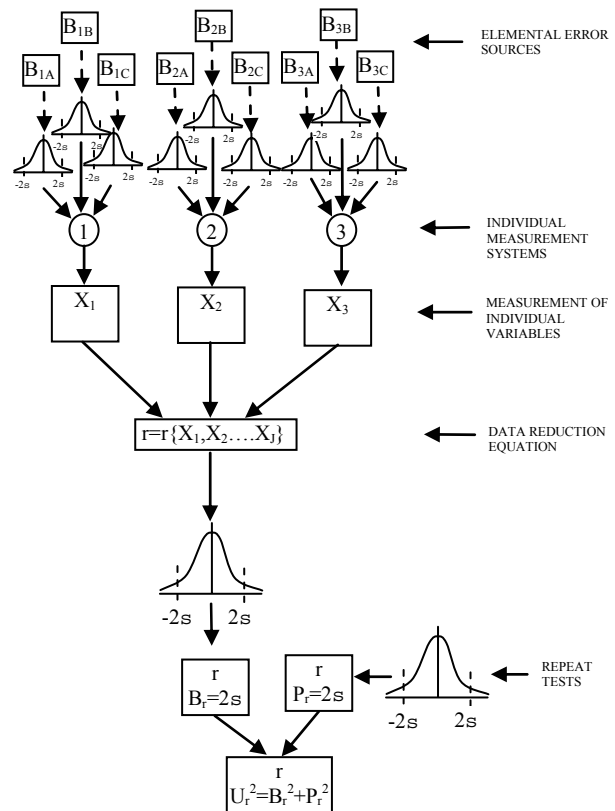

Figure 8.2- Uncertainty assessment methodology by Monte Carlo method.

d) Setup simulations consisting of N number of simulations, in which elemental bias/precision error values are assigned randomly complying with Gaussian error distributions.
e) Calculate the result and its distribution. i.e. calculate mean and standard deviation of result from N simulations.

f) Determine the bias limit by taking twice the standard deviation.

g) Perform repeat tests (minimum 10) and find standard deviation.

h) Take twice the standard deviation to find the precision limit (for 95% confidence).

i) Root-sum-square bias and precision errors to find the total uncertainty limit.

8.3 Uncertainty Analysis for Model Resistance Including Form Factor

Uncertainty in Form Factor by Conventional Method. Model tests for powering prediction consists of resistance tests, self-propulsion tests, and open water propeller tests. Uncertainty in total resistance tests were investigated by the 22nd ITTC Resistance Committee and an example of such procedure was given. This procedure was later updated by the 23rd ITTC Specialist Committee on Procedures for Resistance, Propulsion and Open Water Tests. Although uncertainty in form factor uncertainty was recognized, it was not included in either of the procedures.

The current approach to form factor uncertainty limit estimation makes use of Prohaska's method

Figure 8.3 Form factor is determined from a plot of a regression line, in the form of $y=mx+c$ in which:

$$X_i = \frac{Fn^4}{C_F} \quad \text{and} \quad Y_i = \frac{C_T}{C_F}$$

$$\frac{C_T}{C_F} = \frac{mFn^4}{C_F} + (1+k)$$

where,

$$X_i = \frac{Fn^4}{C_F}, \quad Y_i = \frac{C_T}{C_F}$$

Form factor *(1+k)* is the intercept of the regression, i.e. *c* in the regression line. Hence

the data reduction equation for the form factor becomes:

$$(1+k) = c = f(C_T(Rx, \rho, V, S), C_F(V, L, \upsilon), Fn(V, L))$$

$$c = \frac{\sum_{i=1}^{N} X_i^2 \sum_{i=1}^{N} Y_i - \sum_{i=1}^{N} X_i \sum_{i=1}^{N} X_i Y_i}{N \sum_{i=1}^{N} X_i^2 - \left(\sum_{i=1}^{N} X_i\right)^2}$$
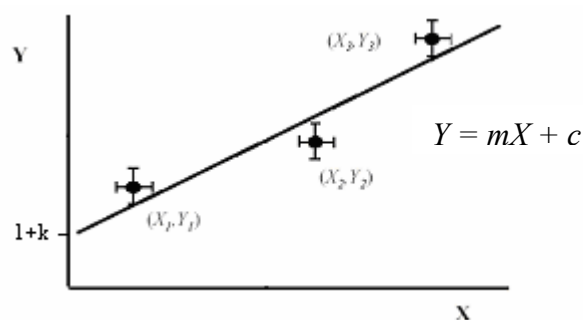

Figure 8.3- Uncertainties in form factor determination.

Uncertainty in *c* can be calculated using Eq. 7.28 of Coleman and Steele (1999) as:

$$Uc^2 = \sum_{i=1}^{N} \left(\frac{\partial c}{\partial Y_i}\right)^2 P_{Y_i}^2 + \sum_{i=1}^{N} \left(\frac{\partial c}{\partial Y_i}\right)^2 P_{X_i}^2$$

$$+ \sum_{i=1}^{N} \left(\frac{\partial c}{\partial Y_i}\right)^2 B_{Y_i}^2 + 2\sum_{i=1}^{N-1}\sum_{k=i+1}^{N} \left(\frac{\partial c}{\partial Y_i}\right)\left(\frac{\partial c}{\partial Y_k}\right) B_{Y_i Y_k}$$

$$\sum_{i=1}^{N} \left(\frac{\partial c}{\partial Y_i}\right)^2 B_{X_i}^2 + 2\sum_{i=1}^{N-1}\sum_{k=i+1}^{N} \left(\frac{\partial c}{\partial X_i}\right)\left(\frac{\partial c}{\partial X_k}\right) B_{X_i X_k}$$

$$+ 2\sum_{i=1}^{N}\sum_{k=1}^{N} \left(\frac{\partial c}{\partial X_i}\right)\left(\frac{\partial c}{\partial Y_k}\right) B_{X_i Y_k}$$

As both Xi and Yi are not direct measurements, but functional relations of common measurements, the correlated systematic uncertainty sources must be taken into account (the full equation is overleaf).

As the data reduction equation is very complex and the task of obtaining partial derivatives is extremely laborious, numerical approximation to the partial derivatives can be utilized for the current purpose. The forward-

differencing finite-difference method was applied to the data reduction equation to obtain partial derivatives by use of a spreadsheet (Insel, Gustafsson and Wiggins 2005). Bias errors were estimated using the same data utilised in the 22nd and 23rd ITTC resistance tests uncertainty example.

$$Uc^2 = \sum_{i=1}^{N}\left(\frac{\partial c}{\partial V_i}\right)^2 P_{V_i}^2 + \sum_{i=1}^{N}\left(\frac{\partial c}{\partial R_i}\right)^2 P_{R_i}^2$$

$$+ \sum_{i=1}^{N}\left(\frac{\partial c}{\partial V_i}\right)^2 B_{V_i}^2 + \sum_{i=1}^{N}\left(\frac{\partial c}{\partial L_i}\right)^2 B_{L_i}^2$$

$$+ \sum_{i=1}^{N}\left(\frac{\partial c}{\partial \upsilon_i}\right)^2 B_{\upsilon_i}^2 + \sum_{i=1}^{N}\left(\frac{\partial c}{\partial R_i}\right)^2 B_{R_i}^2$$

$$+ \sum_{i=1}^{N}\left(\frac{\partial c}{\partial S_i}\right)^2 B_{S_i}^2 + \sum_{i=1}^{N}\left(\frac{\partial c}{\partial \rho_i}\right)^2 B_{\rho_i}^2$$

$$+ 2\sum_{i=1}^{N-1}\sum_{k=i+1}^{N}\left(\frac{\partial c}{\partial V_i}\right)\left(\frac{\partial c}{\partial V_k}\right)B_{V_iV_k}$$

$$+ 2\sum_{i=1}^{N-1}\sum_{k=i+1}^{N}\left(\frac{\partial c}{\partial L_i}\right)\left(\frac{\partial c}{\partial L_k}\right)B_{L_iL_k}$$

$$+ 2\sum_{i=1}^{N-1}\sum_{k=i+1}^{N}\left(\frac{\partial c}{\partial \upsilon_i}\right)\left(\frac{\partial c}{\partial \upsilon_k}\right)B_{\upsilon_i\upsilon_k}$$

$$+ 2\sum_{i=1}^{N-1}\sum_{k=i+1}^{N}\left(\frac{\partial c}{\partial R_i}\right)\left(\frac{\partial c}{\partial R_k}\right)B_{R_iR_k}$$

$$+ 2\sum_{i=1}^{N-1}\sum_{k=i+1}^{N}\left(\frac{\partial c}{\partial S_i}\right)\left(\frac{\partial c}{\partial S_k}\right)B_{S_iS_k}$$

$$+ 2\sum_{i=1}^{N-1}\sum_{k=i+1}^{N}\left(\frac{\partial c}{\partial \rho_i}\right)\left(\frac{\partial c}{\partial \rho_k}\right)B_{\rho_i\rho_k}$$

$$+ 2\sum_{i=1}^{N-1}\sum_{k=i+1}^{N}\left(\frac{\partial c}{\partial L_i}\right)\left(\frac{\partial c}{\partial S_k}\right)B_{L_iS_k}$$

$$+ 2\sum_{i=1}^{N-1}\sum_{k=i+1}^{N}\left(\frac{\partial c}{\partial \upsilon_i}\right)\left(\frac{\partial c}{\partial \rho_k}\right)B_{\upsilon_i\rho_k}$$

Repeat tests were utilized to determine the precision errors (PRX) at various speeds. While PRX varies in magnitude it is almost constant as a percentage of resistance (RX), increasing only slightly as a percentage at the lower speeds. Figure 8.4 compares the actual precision bands found from the repeat tests to those

produced by assuming P_{RX}/R_X is constant. The error due to this assumption is within 0.2 % of k, indicating that a repeat test at one speed can be utilized in the precision error estimation.
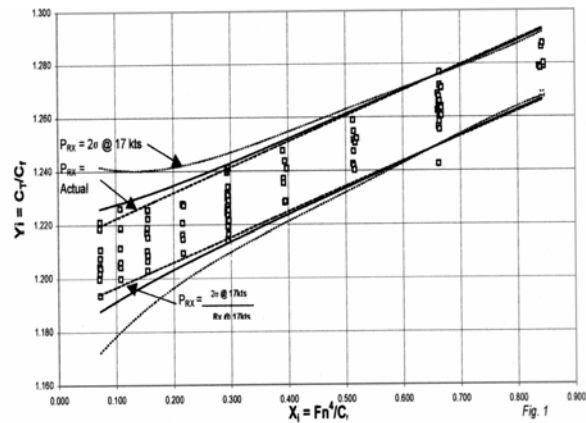

Figure 8.4- Effect of P_{RX} on uncertainty model of Prohaska Plot

Uncertainty in Form Factor by Monte Carlo Methods. Correlations arise due to common bias error sources such as temperature measurement, viscosity etc. As these correlated systematic errors can be calculated easily, two types of calculations were performed as outlined in the previous Section:

a) Without any concern with correlated bias sources, hence all bias errors have their own distribution functions.
b) Using the same distribution functions for correlated systematic errors. For example in the case of form factor all speeds utilize the same model length bias error within each simulation. Hence they are systematically correlated.

The model test results in the ITTC resistance example (ITTC, 2002a) were obtained with a Monte Carlo approach. Firstly 50,000 simulations were run, form factor, and total resistance coefficient results are given below (Figs. 8.5 − 8.8).

During the Monte Carlo analysis the following assumptions were made for correlated bias errors:

▪ Temperature measurement error is a correlated bias error between the runs.

▪ The fresh water density curve fit error is correlated.

▪ Bias error due to use of ρ =1000 is a constant error not a distribution.

▪ The fresh water viscosity formula error is a correlated bias error.

▪ Model length and wetted surface area errors are correlated bias errors.

▪ Model speed bias errors: pulse and count are non-correlated, meanwhile disk diameter error is a correlated bias error.

▪ Resistance measurement calibration weights, transducer calibration, transducer alignment errors are correlated, AD conversion error is an uncorrelated error.
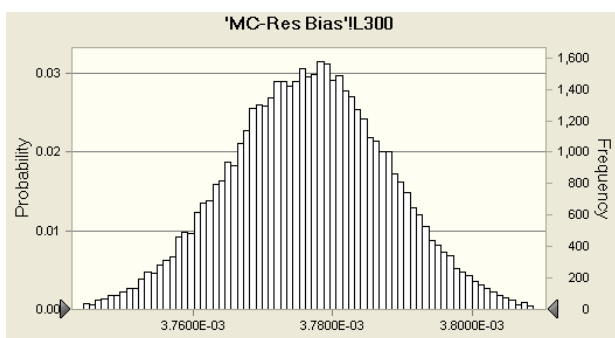

Figure 8.5- Model total resistance coefficient at 17 knots with correlated bias error precautions (Mean: 3.7765 10^{-3}, Std Dev: 0.011545 10^{-3}, i.e. 0.61 % uncertainty).
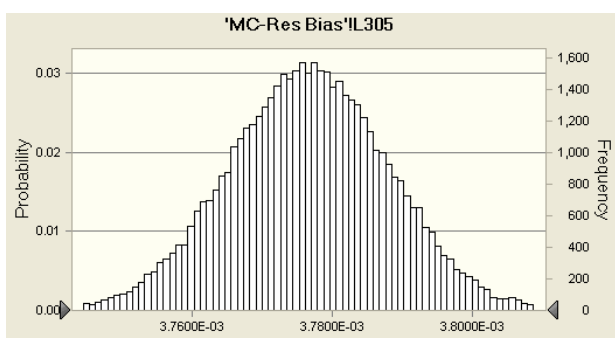

Figure 8.6- Model total resistance coefficient at 17 knots with correlated bias error precautions (Mean: 3.7765 10^{-3} kN, Std Dev: 0.001149 10^{-3}, i.e. 0.61 % uncertainty).
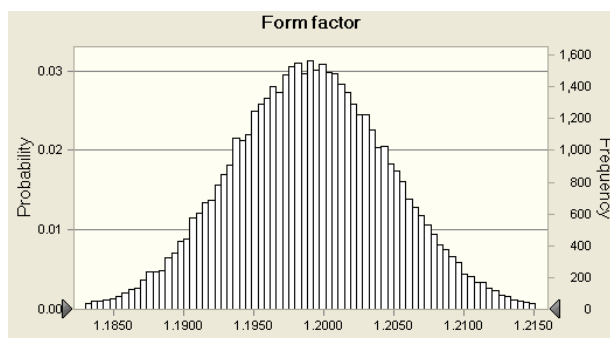

Figure 8.7- Form factor without correlated bias error precautions, (Mean: 1.199, Std Dev: 0.0057 kN, i.e. 5.726 % uncertainty of k).
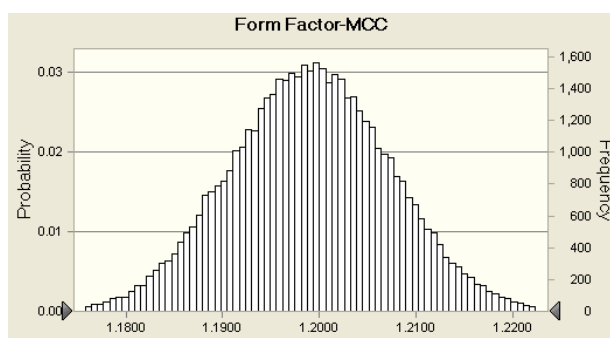

Figure 8.8- Form factor with correlated bias error precautions, (Mean: 1.199 kN, Std Dev: 0.0083 kN, i.e. 8.3417 % uncertainty).

Firstly a comparison of model total resistance coefficient was made. The 23rd ITTC resistance example uncertainty (ITTC 2002) has a value of 0.615 % for the bias error limit. Monte Carlo analysis revealed an uncertainty of 0.612 % for the bias limit. This agreement between the results has indicated that Monte Carlo Methods can be utilised for uncertainty analysis.

Table 8.1- Comparison of uncertainties between conventional and Monte Carlo methods.

Method	Without correlated bias error considerations	With correlated bias error considerations
Conventional	5.553%	8.322 %
Monte Carlo	5.726%	8.3417%

Model total resistance coefficient uncertainty including form factor is given in Figs. 8.9 and 8.10.
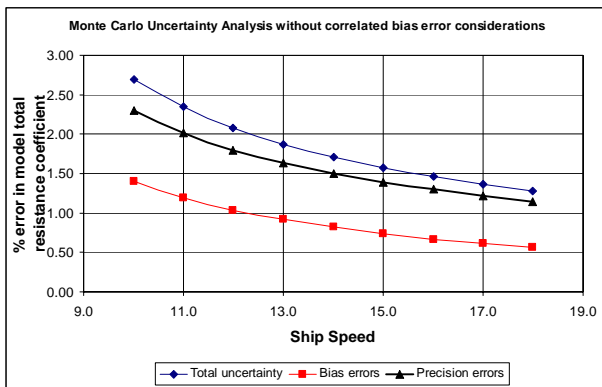
Figure 8.9- Uncertainties across the speed range for the model total resistance coefficient without taking correlated systematic errors into account.
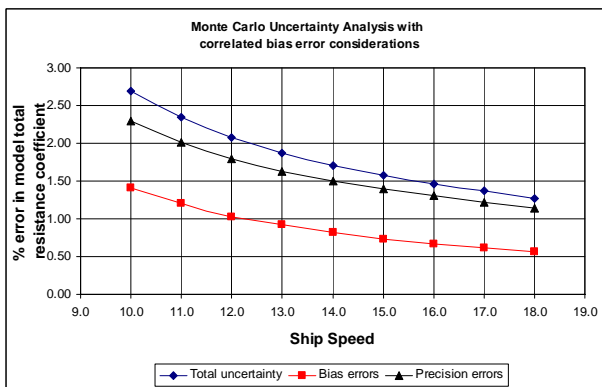

Figure 8.10- Uncertainties across the speed range for the model total resistance coefficient taking correlated systematic errors into account.

Form factor uncertainty with and without correlated bias error corrections are given in Table 8.1. The conventional and Monte Carlo methods agree with each other. Form factor uncertainty is smaller for the case in which no systematic correlation considerations were made. This is somehow unexpected, as systematic correlation consideration should reduce the uncertainty. The random components on the Prohaska plot are reduced when correlated systematic errors are taken into account. This results in a larger change in the form factor.

The uncertainty found using Prohaska's method in the analysis above covers only the errors associated with the conduct and analysis of the experimental data. It does not address the uncertainty (or applicability) of the method itself.

8.4 Uncertainty Analysis – Extrapolation

Extrapolation procedures are complex and involve many steps, some of which were originally meant to be solved graphically. Setting up the data reduction equations and propagating the errors in an extrapolation method can be done, but becomes unwieldy in practice. Also, the most important issues affecting uncertainty, such as those involved in assessing form factor, in selecting a friction line or in scaling the wake, have very little to do with the (numerical) propagation of errors through an uncertainty analysis and everything to do with understanding of the issues and technical judgment. Hence it was decided that one approach to assessing uncertainty in the extrapolation process was to carry out a Monte Carlo simulation of the variation in inputs and assess the resulting uncertainty in the ship powering prediction. This was done for two main extrapolations: an extrapolation using a self-propulsion test only; and the ITTC 1978 extrapolation method. The results are presented for selected examples from the database of ship and full scale trials data and are shown as percentage variation in the predicted ship power.

In the approach, the analysis of which was done by Molloy (2005), the measured input values obtained from model tests were varied arbitrarily by 1% and the sensitivity of the predicted power to these variations was assessed. Each input value was examined individually and in combination with other factors. While this approach does not assess the actual uncertainty level in a particular case (which can be obtained from a complete uncertainty analysis of the actual tests), it gives insight into the behaviour of the method as a whole and identifies the major sources of instability. As expected, combination of uncertainty from multiple sources is cumulative.

Uncertainty in the ITTC 1978 Method. First of all each of the results from the model tests were arbitrarily assumed to vary such that the distribution of the variation was normal and a standard deviation of 1% of the variation of the nominal measured value was chosen. The parameters varied are shown in Table 4.2. The simulation was run for 10,000 iterations, in which each of the input test parameters was varied randomly within the range stipulated.

Table 4.2- Parameters varied.

Tests	Parameters varied	% Variation
Self-propulsion test	V_M, n_M, T_M, Q_M, F_D	1%
Resistance Test	R_{TM}, V_M	1%
Propeller open water test	K_T, K_Q, J	1%

The form factor was set to zero and no correlation allowances were used. The full scale operating parameters of ship delivered power, revolutions, thrust and torque were predicted. The approach was repeated for several different ships of the data set described in Section 7.1 (see Table 8.3). The results are plotted in Fig. 8.11. The standard deviation in the full scale ship delivered power values was found to be in the range 1.6-5.3% for the vessels studied. The standard deviations in revolutions, propeller thrust and torque were in the ranges of 0.8%-1.5%, 1.5%-7% and 1.4%-4% respectively, Table 8.4 (Molloy 2005). Note that these results are for an arbitrarily varied standard deviation of 1% in the input parameters and that the approach is also somewhat conservative since no account was taken of cross correlated bias limits in the analysis (see Section 8.3). Note that the ship represented by ITTC #8 has a larger sensitivity to the variation in results of the tests. This may be an outlier, but with only ten ships analysed, it is impossible to make a definitive conclusion on this at this stage. Also for this ship, as for several others in the data set, the thrust deduction fraction is larger than the wake fraction and this leads to problems in applying the ITTC 1978 wake scaling formula.

Total uncertainty is in line with the other ships (see later).

Table 8.3- Predicted Power Variation with Variation of All Test Inputs.

Chart Legend	Database ship number	Ship Type	# of Props	Ship Speed
ITTC #1	03	Passenger	2	10.26 m/s
ITTC #2	25	Passenger Cruise Liner	2	8.49m/s
ITTC #3	33	Passenger	2	11.32 m/s
ITTC #4	52	RoRo Ferry	2	10.29 m/s
ITTC #5	70	Passenger Cruise Liner	2	12.35 m/s
ITTC #6	76	Chemical Carrier	1	7.36m/s
ITTC #7	SNO6	Single	1	8.23m/s
ITTC #8	R-Class	R-Class Icebreaker	2	8.75m/s
ITTC #9	SSMB_SuezMax		1	8.74m/s
ITTC #10	SSMB_VLCC		1	8.48m/s

In the second study, variation in each of the experiments was done individually. Summarising, it was found (Molloy 2005; Molloy et al. 2005) that the standard deviations in predicted delivered power were normally in the range up to 2-3% when only the inputs from the resistance test OR propeller open water test were assumed to vary with a standard deviation of 1%, Fig. 8.12, but that predicted power variation had a standard deviation of up to 5-6% when the inputs from only the self-propulsion test were assumed to vary with a standard deviation of 1%. For two ships of the database, the results of this are shown in Figs. 8.12 and 8.13.

Further study showed that it was the variation in the velocity value in the self-propulsion test that impacted the overall uncertainty most strongly (Molloy et al. 2005) and this was ascertained to be because uncertainty in the velocity value of the ship self propulsion point impacted the estimation of ship resistance coef-

ficient, thrust deduction fraction, wake fraction and the determination of the ship propeller operating point. The method could almost be described as rather ill-conditioned or unstable

for one ship since a variation in velocity with a 1% standard deviation resulted in a standard deviation in delivered power of up to 5 and 6% for this ship. Results are shown in Fig. 8.13.
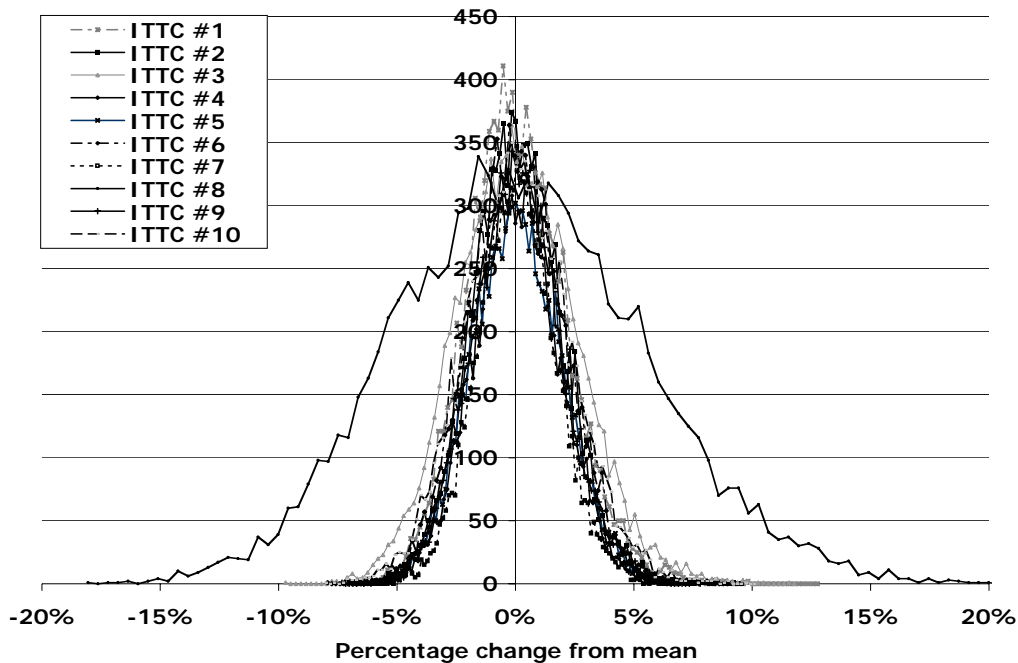

Figure 8.11- Variation in predicted ship delivered power for several ships using the ITTC 1978 extrapolation method and a Monte Carlo simulation.

Table 8.4- Comparison of Standard Deviations of Predicted Parameters.

All test inputs varied by 1%								
Ship	**V_S** (m/s)	**N_S** (rps)	**P_{DS}** (kW)	**T_S** (N)	**$Q_{S - Port}$** (Nm)	**$Q_{S - St'd}$** (Nm)	**$Q_{S - Average}$** (Nm)	**P_{ES}** (kW)
ITTC #1	1.01%	1.43%	2.10%	2.54%	1.41%	1.41%	1.47%	6.07%
ITTC #2	1.00%	1.17%	1.89%	2.62%	1.55%	1.55%	1.53%	5.91%
ITTC #3	1.00%	1.48%	2.52%	1.97%	2.13%	2.13%	2.20%	5.45%
ITTC #4	1.00%	1.05%	1.81%	2.28%	1.50%	1.50%	1.27%	5.07%
ITTC #5	0.99%	1.30%	1.91%	2.18%	1.81%	1.81%	1.65%	5.24%
ITTC #6	1.00%	0.86%	2.03%	1.55%	1.66%			4.08%
ITTC #7	1.00%	0.84%	1.65%	7.18%	1.43%			4.36%
ITTC #8	1.00%	1.35%	5.32%	2.53%	4.08%	4.08%	3.94%	4.08%
ITTC #9	1.00%	1.06%	1.86%	5.08%	1.80%			4.95%
ITTC #10	1.02%	0.90%	2.27%	5.13%	2.42%			4.11%

Perhaps greater interest arises from uncertainty in the form factor, friction line, wake scaling approach and correlation allowance.

▪ Uncertainty in the correlation allowance can be estimated from a "best guess" based on

knowledge of how values of correlation allowance at an institution have been assembled. At worst this might be ±0.0004, but would drop for ship types for which the institution had considerable prior knowledge. Some values for this may result from the variations in correlation

allowance found from analysis of the ships represented in the database of model tests and trials results collected by this Committee, but the Committee was not able to complete this work during its tenure. (For example see Fig. 7.4).

- Uncertainty in the form factor might be obtained from uncertainty in the intercept of the Prohaska type plot used to obtain the values and one approach to this problem has been described in Section 8.3. This does not address uncertainty in the approach to obtain form factor, or in whether a form factor should be used or not (the latter might be estimated as $\pm k$ and can probably be taken as the extreme of uncertainty associated with use of form factor).

- Uncertainty in the friction line can also be interpreted in several ways. It might be taken as

an estimate in uncertainty in the line itself assuming that the line is the correct representation of turbulent flat plate data (some idea of this might be obtained by assessing uncertainty in the original data making up the curve fit). Alternatively it might be estimated in the extreme case by taking a value based on $\pm$ the difference between different lines (e.g. between the ITTC line and a turbulent flat plate friction line, or between different flat plate friction lines). This difference changes with Reynolds number.

- The uncertainty in wake scaling can be large, as limited data exists, and might be based on regression formulae from data on similar vessels (if this is available). The uncertainty reduces as available data banks of trials data and model experiments are increased.
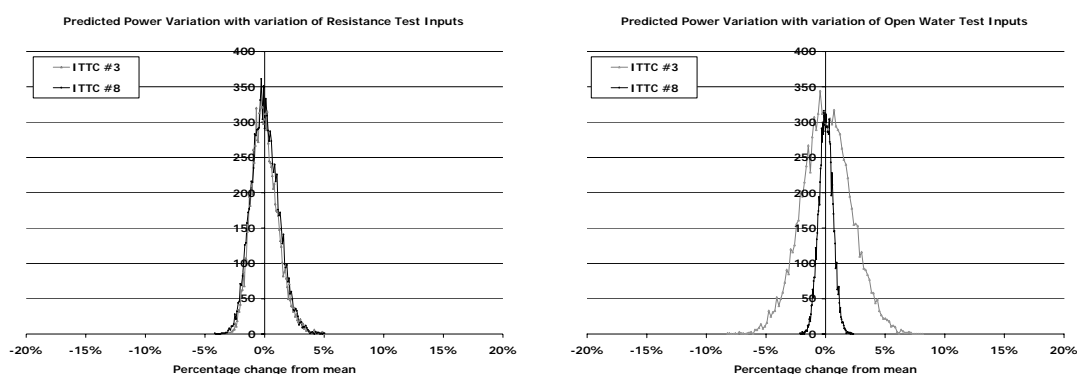

Figure 8.12- Variation in predicted delivered power for two ships using the ITTC 1978 method with variations only in inputs from the resistance test and then only inputs from the propeller open water test.
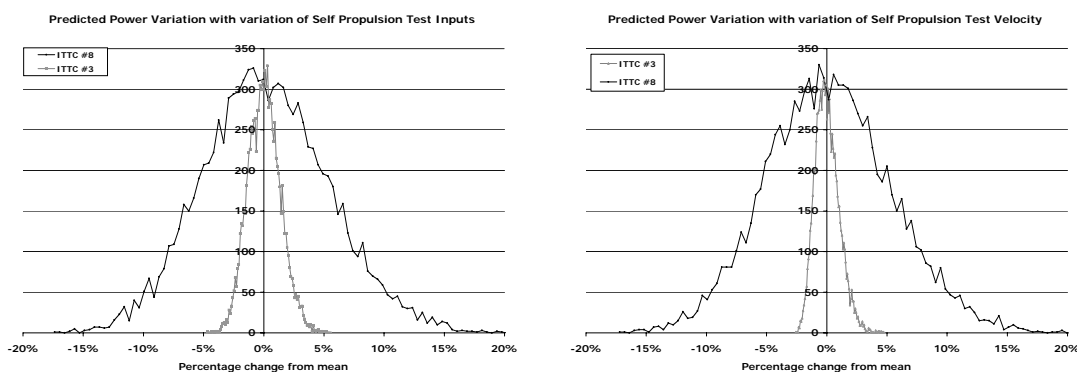

Figure 8.13- Variation in predicted delivered power for two ships using the ITTC 1978 method and variations in all self-propulsion test inputs as well as variation in velocity only (second plot).

A similar approach to that used for variation in the input parameters from the various test results was used to assess the effect of variation in wake, form factor and friction line, Fig. 8.14 (Molloy 2005). Here the standard deviation of the variation in friction line was taken to be ½ the difference between the ITTC 1957 line and a flat plate turbulent friction line (in this case the Grigson line was used). The form factor was varied by assuming a standard deviation of 10% in the form factor; for the vessel represented by ITTC#8, the form factor was 0.4 and the standard deviation in the variation was taken as 0.04. The wakes were varied by 4-12%, the standard deviation taken as approximately ½ the difference between the wake of the model and the wake of the ship calculated using the traditional ITTC 1978 method. Figure 8.15 shows the variation in predicted power when all inputs from tests are input and variation is assumed in friction line and wakes.

Extrapolation Using Self Propulsion Tests Only. In this study (Molloy 2005), extrapolation was done using only the results from self-propulsion tests (designated here as E2001). The method is outlined in Section 5.3 of this report and has been presented previously by Holtrop (2001) and Molloy/Bose (Molloy 2001; Molloy and Bose 2001; Bose and Molloy 2001). The results are shown for one ship in Fig. 8.16 for standard deviations of 1% in all input parameters from each model test as well as uncertainty in form factor (±10%), friction line (±1/2 the difference between lines as described above) and wake scaling. The wake scaling factor was taken as 0.97 with a standard deviation of the variation of 0.03. In the same plot the variation in the equivalent calculation using the ITTC 1978 method is shown. The analysis indicates that, for this ship, overall uncertainty in powering prediction is greater for the ITTC 1978 extrapolation method (approximately double) than for an extrapolation based only on load varied self-propulsion tests, Table 8.5. This is because a greater number of inputs and experiments are employed in the ITTC 1978 method and because uncertainty in

the velocity value of the ship self propulsion point in the ITTC 1978 method had a greater impact on the estimation of ship resistance coefficient, thrust deduction fraction, wake fraction and the determination of the ship propeller operating point using Eq. 8.1, than in the method using self-propulsion tests only which uses Eq. 8.2 to determine the ship operating point.
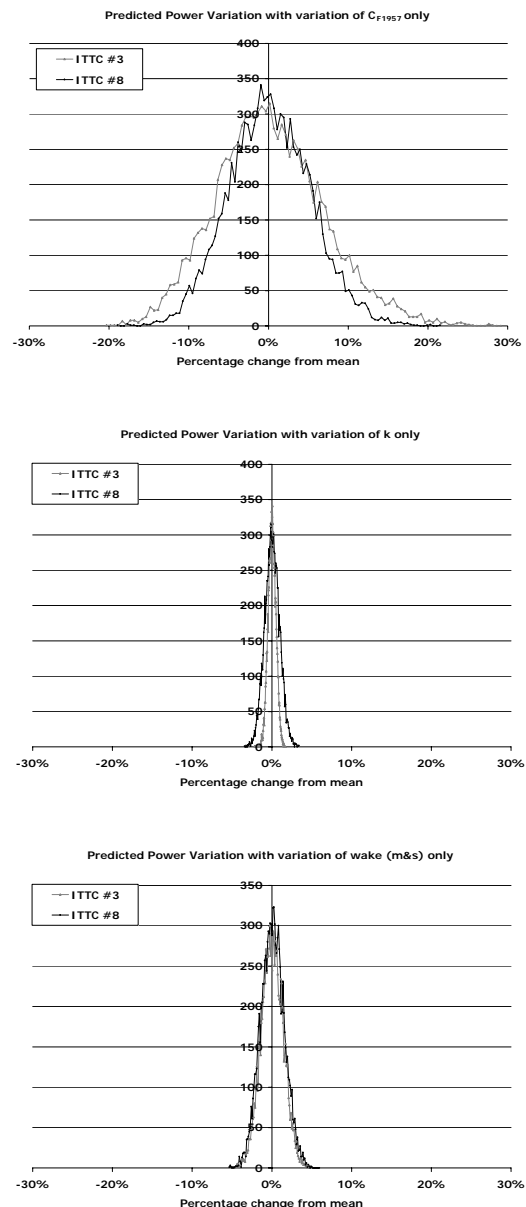

Figure 8.14- Variation in predicted delivered power for two ships using the ITTC 1978 method as a result of variation in friction line, form factor and wake.
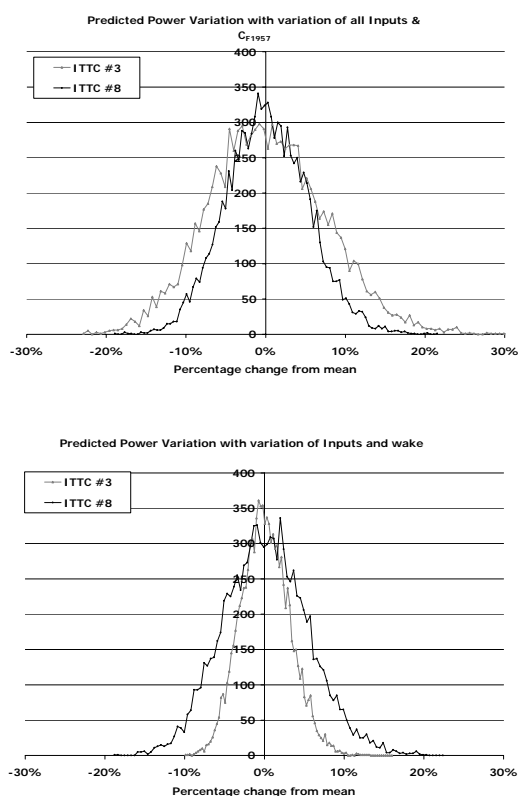
Figure 8.15- Variation in predicted power for two ships using the ITTC 1978 method first assuming variations in all test inputs as well as in friction line and then in all test inputs and wake.

$$\frac{K_{TS}}{J^2} = \frac{S_s}{2D_S^2} \frac{C_{TS}}{(1-t)(1-w_{TS})^2} \qquad (8.1)$$

$$\frac{K_{TS}}{J^2} = \frac{T_{TS}}{\rho_S D_S V_S^2} \qquad (8.2)$$

Concluding Remarks of This Section. This Section shows that uncertainty in the extrapo-

lation method is substantial, but that certain aspects of the extrapolation process, or the nature of the extrapolation process itself, can have a large influence on uncertainty.

Uncertainty in the values calculated from the friction line leads to large uncertainty in ship powering prediction. The question arises as to how certain is our knowledge of the friction coefficients represented by the turbulent flat plate friction lines. Here the variation was considered to be represented by a standard deviation of ±½ the difference between the ITTC 1957 line and the Grigson line, which is probably about as high as it is likely to be since other lines lie between these two. Of the uncertainty in the results from the tests, results from the self propulsion tests, especially uncertainty in velocity values from those tests, has the largest effect on uncertainty in ship powering prediction, at least for some ships.

Generally, the following factors had a smaller influence on uncertainty levels in the ship powering performance extrapolation process: variation in results from model tests; small variations in form factor on the order of ±10%; and variations in wake scaling from model to full scale. For the form factor, our knowledge may be better represented by considering a variation of ±100% of the form factor, or ±50% about a mean value of $k/2$, since that would represent uncertainty in the form factor approach completely. However, that study has not yet been completed.

Table 8.5- Variation in powering outputs for two ships of the database and for two extrapolation methods for one of these ships.

% Standard Deviation	Vs	Ns	PDs	Ts	Qs - Port	Qs – Stb'd	Qs – Ave.	Pes
	(m/s)	(rps)	(kW)	(N)	(Nm)	(Nm)	(Nm)	(kW)
ITTC #3								
ITTC 1978	0.00%	0.70%	6.85%	2.91%	6.33%	6.33%	4.62%	3.59%
ITTC #8								
ITTC 1978	0.99%	1.79%	7.37%	3.63%	6.70%	6.70%	8.41%	6.59%
E2001	1.01%	1.63%	3.60%	2.36%	2.37%	2.36%	1.53%	3.49%

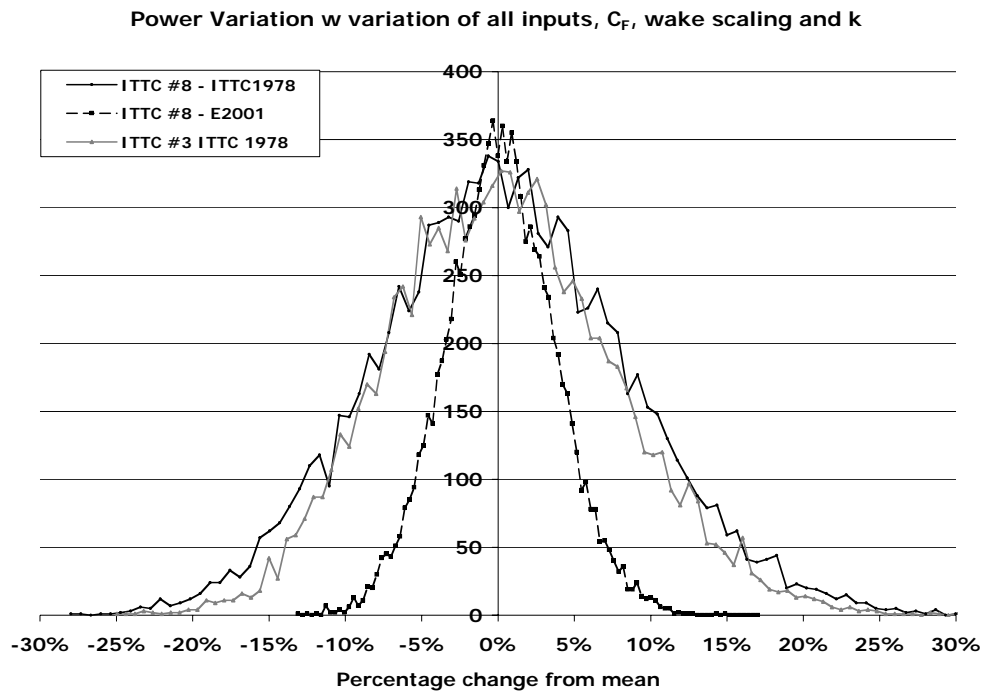**Power Variation w variation of all inputs, C_F, wake scaling and k**

Figure 8.16- Comparison of the variation in predicted ship delivered power for two ships using the ITTC 1978 extrapolation method and one ship using a method based only on the results from self-propulsion tests (designated E2001).

Uncertainty in ship powering prediction using the ITTC 1978 extrapolation method itself is larger than (approximately double) that from an extrapolation method which uses results from load-varied self-propulsion tests only, at least for the ship for which load varied self-propulsion test data were available. This is because: a greater number of inputs and experiments are employed in the ITTC 1978 method; and the method used to obtain the ship propeller operating point uses the value of ship thrust directly rather than the ship resistance coefficient, wake fraction and thrust deduction fraction as it does in the ITTC 1978 method. The ship thrust is scaled directly from the model thrust which is obtained from a linear plot of towing force against propeller thrust. More test cases (ship datasets) are needed to validate this conclusion.

There are also differences shown between sets of data (different ships). For example, one ship (ITTC#8) showed a predicted power that was much more sensitive to variation in the model test results than the other data sets stud-

ied (standard deviation of 5.3% versus values in the range 1.6-2.5% when the uncertainty in the friction line is not included) and this arose primarily from sensitivity to variation in results from the self-propulsion tests. The ship represented by data set ITTC#3 showed much larger sensitivity to uncertainty in the results from the propeller open water test results than ITTC#8. Also, the wake scaling method used in the ITTC 1978 method should be reformulated especially for ships where the thrust deduction fraction may be bigger than the wake fraction.

8.5 Uncertainty Analysis in Speed/Powering Trials

The uncertainty assessment in measurements during sea trials was outlined by the 23rd ITTC Specialist Committee on Speed and Powering Trials.

However, it is rarely possible to conduct the trials at contract conditions, as speed/powering trials are often conducted within a limited time

scale. Measured ship speed and shaft power must be corrected for the differences between trial conditions and the contract conditions. Hence ship trial results have uncertainties mainly due to two sources:

- Trial measurements: torque, shaft rate of revolution, ship speed measurement uncertainty
- Trial analysis: mainly corrections applied to trial measurements.

An attempt to understand the magnitudes of these errors was made through analysis for a set of speed/powering trials with a series of 12 twin screw sister vessels. Each trial consists of 5 pairs of runs in opposite directions and was conducted in different environmental conditions. Hence the whole set of trial results include errors due to measurement, hull form production, corrections for environmental conditions.

Each run in a trial was analysed and corrected according to the Procedure outlined in ITTC Standard Procedure 7.5-04-01-01.2. Elemental bias error sources were taken similar to the method given by the 23rd ITTC. However Monte Carlo methods were utilised for uncertainty estimations, as data reduction equations are complicated.

Bias errors in a single run originate from measurements and corrections for environmental conditions. A number of basic measurements are conducted during the trials for both analysis and corrections. The bias error limits in each measurement should be determined by using the basic principles.

Ship Conditions. In order to define the ship loading, fore and aft draughts are measured. The draught marks at the perpendiculars are read by eye before departing on the trials. Depending on the sea conditions, a reading error of ±2 cm can be assumed. Ship dimensions are also affected by the production errors. In the current work ± 10 cm in the ship length and ± 2 cm in the ship breadth were assumed as bias errors in dimensions. Block coefficient error

was accepted as 0.001. Hence the error in the displacement can be calculated through the displacement equation:

$$\Delta = \rho * g * C_B * L * B * T$$

Environmental Conditions. Water temperature and salt content is also required if they are different from contract conditions. Water temperature is measured with a thermometer and best accuracy in trial conditions can be assumed 0.5°C. This error is to be a combination of measurement and temperature changes in the trial area. Salt content is usually assumed to be constant at the trial site, however in case of no measurements a bias error limit of 0.005 in density due to salt content uncertainty was assumed in the current work.

Shaft Torque Measurement. In the trials under consideration, shaft torque measurements were generally conducted with a full bridge strain gauge rosette excited with a battery box and amplified with a purpose built amplifier-decoder and transmitted to a stationary receiver through antenna as shown in Fig. 8.17.
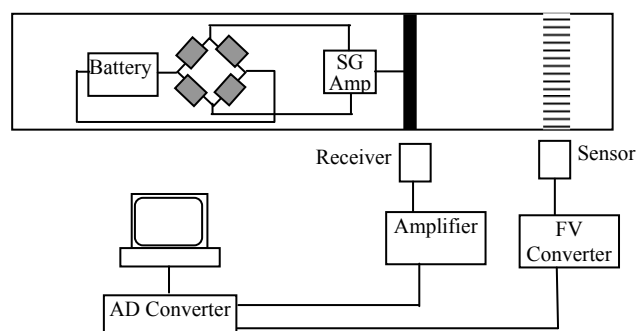

Figure 8.17- Shaft torque and rate of revolution measurements

Calibration is performed by placing a shunt resistor (R_{CAL}) into one of the arms of strain gauge bridge which simulates corresponding strain as:

$$\varepsilon_{CAL} = \frac{1}{4k} \frac{R}{R + R_{CAL}}$$

During measurements, resistance of Wheatstone bridge changes with shaft strain in the form:

$$\varepsilon = \frac{1}{k}\frac{\Delta R}{4R}$$

The torque can be calculated from

$$Q = \frac{4GI\varepsilon}{D}$$

where,

$$I = \frac{\pi(D^4 - d^4)}{32}$$

The uncertainty of this measurement system consists of elemental error sources based on:

- Strain gauge
- Calibration of measurement system
- Installation on a ship
- Calculation of torque

Strain Gauge Bridge: In this example, a strain gauge rosette consists of four equivalent strain gauges with specification of

Gauge type   CEA-06-25μs-350 Ω
Gauge resistance Rg=350.0 ±0.4% Ω
Gauge factor at 24 °C 2.045±0.4%
Hence bias errors:
Gauge resistance: B_{Rg}= ±0.4*350/100= ±1.4 Ω
Gauge factor at 24 °C:
B_{Rgf}=±0.4*2.045/100=0.00818

Measured Value Transmitter and Receiver: In this example transmitter and receiver specifications are

Transmitter type: MT 2555A
Receiver type: EV 2510
Bridge supply voltage: 9 V
Nominal input signal: ±2mV/V
Sensitivity, output frequency: Δf=5kHz±25 Hz (±0.5%)
Effect of ambient temperature on sensitivity: ±0.1%
Hence bias errors:
Sensitivity bias: B_{TR1}=25 Hz

Sensitivity due to ambient temp: B_{TR2} = 0.1*5000/100 = 5 Hz

Amplifier Plug in Module: In this example an amplifier was utilized to amplify voltage output to digital/analogue conversion range. Specifications are:
Amplifier type: MD 60C
Measurement range: ±5kHz
Measured value nominal voltage: ±10 V
Linearity deviation: 0.02 %
Residual ripple and disturbing peaks:±0.3 %
Effect of temperature on sensitivity: ±0.1 %
Effect of change in supply voltage: 0.01%

Analogue Digital Conversion Error: In this example data from amplifier was fed into an analogue/digital converter with 12 bit accuracy and ±10 V range. Error in a typical analogue digital conversion is 1.5 bits. Hence bias error in Analogue Digital conversion is:

$$B_{ADC} = \frac{1.5}{2048}10 = 0.0732\,V$$

Calibration Uncertainty: Here a standard resistor is utilized for the calibration of shaft torque measurement. This resistor, shunt resistor, is connected instead of a strain gauge in the full bridge to create a resistance change effect in the measurement chain. The standard calibration resistor in this example has an error not more than 0.01 %. The shaft relative strain ε is obtained from:

$$\varepsilon = \left(\frac{R_1}{R_1 + R_{CAL}}\right)\frac{1}{4k_1} \text{ or } \varepsilon = \frac{R_1}{4k_1 R_2}$$

where,
$$R_2 = R_1 + R_{CAL}$$
R_1 : strain gauge effective resistance
k_1 : gauge factor at 75 °F
R_{CAL} : resistance of the standard resistor

Installation on a ship: Installation in the ship has elemental error sources due to alignment of strain gauge with shaft axis. The 22nd ITTC has given alignment error as:

$$\varepsilon_\alpha = \varepsilon \cos(2\alpha)$$

Calculation of torque: The diameter of the ship shaft can be determined from certification of the shaft, for the current case, a bias limit of ±0.5 mm was utilised for both outside and inside diameter. The bias error in shear modulus depends on the material of the shaft. For the current case 1.15% as specified in the 23rd ITTC was utilised.

Shaft Rate of Revolution Measurements. Shaft speed measurements are made with optical or magnetic pulse generators, a sensor and an amplifier. The number of pulses are counted for a predetermined time and divided into number pulses per revolution to find the shaft rate of revolution.

$$n = \frac{Count}{N * Time}$$

where,
N: number pulses per revolution

Bias error in pulse count is 1 pulse, there is no uncertainty in N. As the time window gets larger the bias error associated with shaft rate of revolution drops. For the current work, the time window is taken as 1 second as power is calculated every seconds.

Ship Speed Measurements. Ship speed is nowadays measured by dGPS systems, and can be calculated by different methods (ITTC 2002b). The most common method for ship speed calculation is to determine the run start position and run end positions, and divide the distance between the two by time elapsed. The uncertainty in time measurement is negligible, the positional bias error limit is about 3 to 5 meters.

Uncertainty due to Shallow Water Correction. The shallow water method correction given by Lackenby (1962) is utilized. The speed loss is given as:

$$\frac{\Delta V_S}{V_S} = 0.1242(\frac{A_M}{H^2} - 0.05) + 1.0 - \tanh(\frac{gH}{V_S{}^2})$$

where,
H : Water depth in m
A_M : Midship section area under water in m^2
ΔV_S : Speed loss due to shallow water in m/s
V_S : Ship speed in m/s

Water depth bias error was accepted as ±2 m. Bias error in midship section area originates from bias errors in breadth, draught and midship section area coefficient which is assumed to be within 0.001. Bias error on ship speed follows the procedure given above.

Wind and Wave Corrections. Wind corrections and wave corrections are based on wind speed, wind direction, wave height, and wave direction.

Wind Correction:

$$RAA = \frac{\rho_A}{2} V_{WR}{}^2 A_{XV} C_{AA}(\psi_{AA})$$

Wave Correction:

$$dR_0 = 0.64 H_{V^2} C_B \frac{B^2}{L} g \rho_{TRIAL}$$

$$dR = dR0[0.667 + 0.333\cos(\alpha)]$$

The current set of data includes Beaufort scale and wind direction values only. Hence a relation between Beaufort scale and wind speed and wave height was established by fitting curves for both variables. SEE error was derived and used in the uncertainty analysis. Beaufort scale is normally estimated by expert opinion; hence a bias error limit of 1 was accepted in the current study.

Wind and wave directions were assumed to coincide in the current work. Wind direction and wave direction bias error limits were estimated as 10 degrees, the course estimation bias error limit was taken as 4 degrees.

Displacement Correction. The ISO 15016 recommendation for displacement correction was utilised

$$R_{ADIS} = 0.65 R_T \left(\frac{\Delta_{TRIAL}}{\Delta} - 1 \right)$$

Contract displacement did not include any uncertainty. Meanwhile trial displacement bias error is explained above.

Water Temperature and Salt Content. The water temperature correction was the same as ISO 15016.

$$R_{AS} = R_{T0} \left(1 - \frac{\rho_{TRIAL}}{\rho} \right) - R_F \left(1 - \frac{C_F}{C_{F-TRIAL}} \right)$$

Density has elemental errors due to temperature measurement, temperature-density fit error, and salt content error. Frictional resistance errors originate from viscosity, length and speed.

Environmental conditions of the current set were various as given in Table 8.6. The results of corrected trials are given in Fig. 8.18.

Table 8.6- Environmental conditions for the trials.

Trial Set	Water depth/Ship length	Wind - Beaufort	Trial disp/ Contract disp	Water temperature	Run time (s)
7	0.145	4	0.935	15.1	294
21	0.301	3	0.966	8.7	477
28	0.186	2.6	0.932	15.1	474
29	0.346	3.5	0.882	5	366
31	0.320	7	0.901	18	557
33	0.246	6	0.876	15.9	600
35	0.190	6.5	0.962	13	600
37	0.331	5	0.963	12.3	601
56	0.323	6	0.884	5	601
63	0.346	0	0.885	4.4	600
87	0.323	4	0.915	11	432
95	0.176	6	0.948	4.5	600

Total Bias Error. Uncertainty in each run was analysed separately, Gaussian distributions

were set up for each elemental bias error sources. If correlated bias errors were applicable, then the same distribution was used for the all runs of the trial. For example the same temperature measurement bias error was applied into all runs.
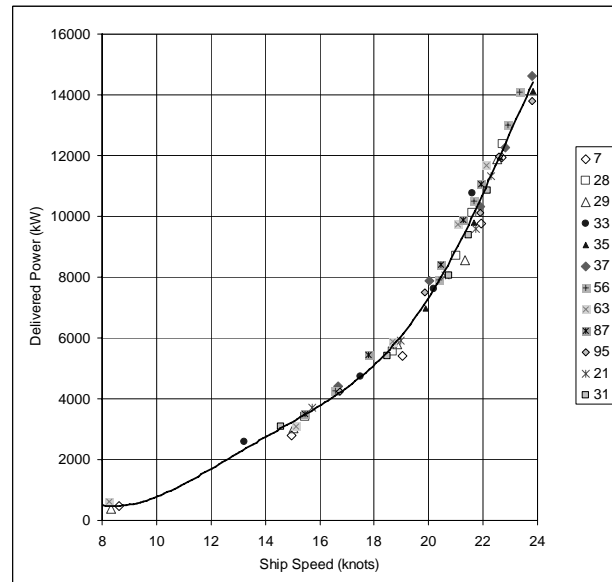

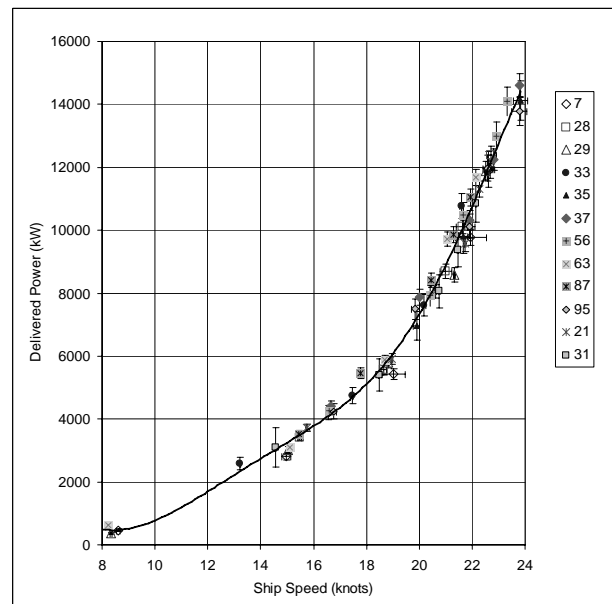Figure 8.18- Result of 12 sets of speed/powering trials.

Figure 8.19- Result of 12 sets of speed/powering trials.

The results of trials are plotted in Fig. 8.19 with error bars defined by bias error limits.

Bias error limits are plotted by dividing the third power of speed in Fig. 8.20 to reduce the effects of speed. A linear curve fit was applied to these bias error limits to represent the whole set of trials.
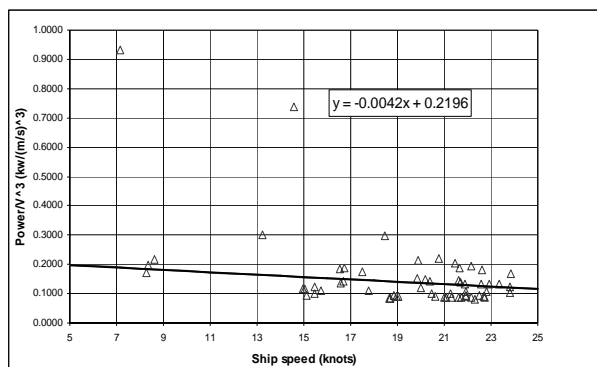

Figure 8.20- Bias errors in trials.

Precision Errors of Trials. Precision errors were defined as the difference between a trial result and the curve fit value at that speed. Then these errors were separated into groups for each 1 knot speed intervals within the speed range. The precision errors were divided by third power of speed, and their standard deviation values were calculated for each speed group and given in Table 8.7 and Fig. 8.21. Average standard deviation was found to be approximately 0.3. Hence precision error at each speed range was accepted equal to twice the mean standard deviation (i.e. $2* 0.3*V^3$).

Table 8.7- Number of trial pairs and standard deviation of trial pairs.

Ship speed (knots)	No of trial pairs	Stdev
15-16	5	0.30887
16-17	4	0.13574
17-18	2	0.44679
18-19	5	0.13802
19-20	3	0.53653
20-21	6	0.31009
21-22	14	0.41375
22-23	10	0.18008
23-24	4	0.29896

The 95% confidence level was plotted in Fig. 8.22 by taking root-sum-square of bias and

precision error limits. Precision and bias error uncertainties are plotted as percentage of power in Fig. 8.23. Precision errors are larger than the bias errors for the data set. As speed increases both bias errors and precision errors drop. Bias errors are less than 5% for all the speed range and about 3 % for the design speed. Meanwhile precision errors are about 9% at lower speeds and about 7 % at the design speed.
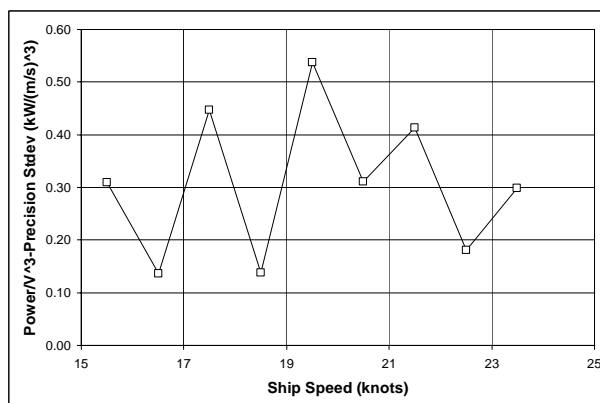

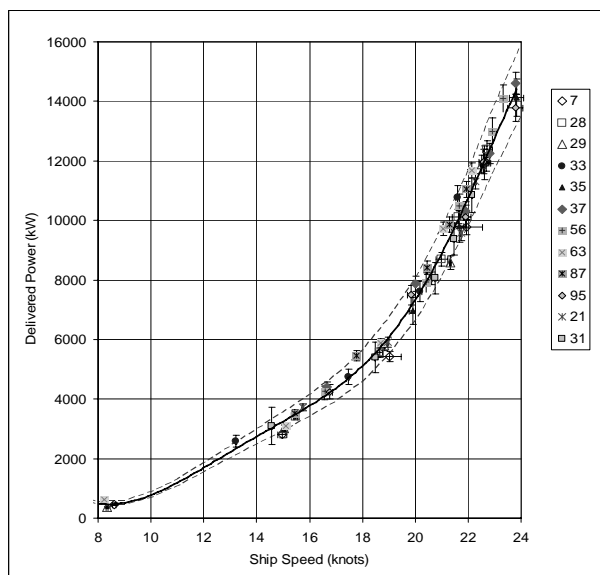Figure 8.21- Standard deviation distribution for 1 knot segments.

Figure 8.22- Total error in sea trials.

The precision errors determined here include the precision errors due to production, environmental conditions and measurements. The choice of correction methods could affect bias and precision error limits, but it should not change the total uncertainty of the trials. Hence

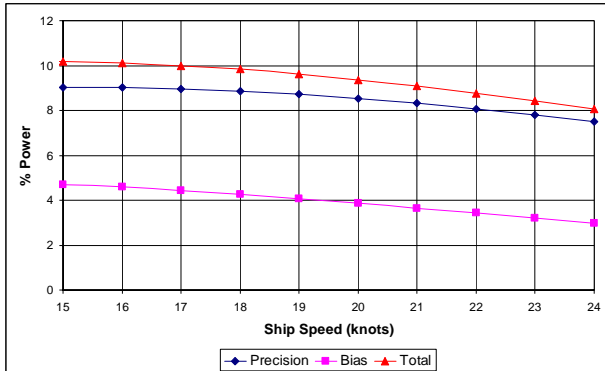very careful consideration should be given to minimise the environmental effects for lower uncertainty.

Figure 8.23- Percentage error in sea trials.

9.   POWERING MARGINS

Matsubara (1995), NYK Line, remarked that sea margin analyses by use of abstract log data are a time-consuming and thankless task. He explained that although he and his predecessor Ishii (1975) worked hard and presented sea margin values shown by the ● and ▲ marks in Fig. 9.1, it seems very difficult to obtain design improvements of actual performance at sea through the examination of sea margins.
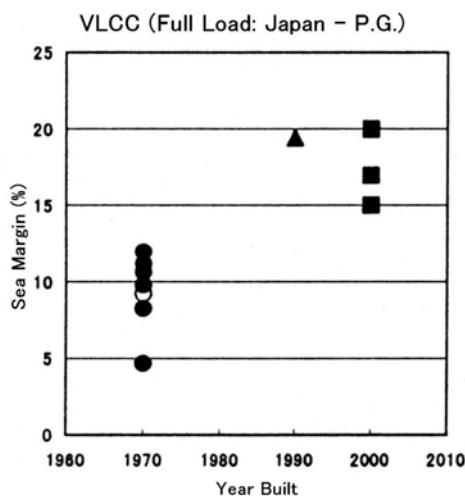

Figure 9.1- Sea Margin Values of VLCCs.

Matsumoto (2003) added the data shown by the ■ marks in Fig. 9.1. The increasing trend of

sea margin allowances is clearly observed. According to Matsumoto, the fuel consumption rate has been decreased by about 70% for VLCCs in the 1990's from those in the 1970's (before the oil crisis), as shown in Fig. 9.2. The rapid decrease of fuel consumption is mainly attained by two facts, namely the change of main engine from turbine to diesel and the adoption of energy saving hull forms.
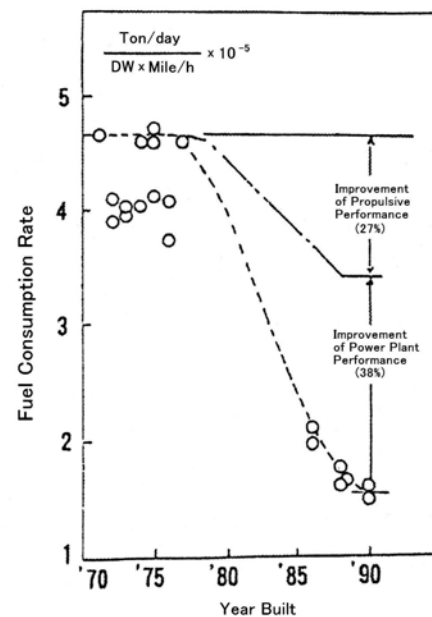

Figure 9.2- Trend of Fuel Consumption of VLCCs.

This means that propulsive power in calm water dropped significantly over these 20 years. Then, as Takahashi and Asai (1985) explained, the power margin ratio must be increased if the ship is to maintain the same speed at sea as in calm water, because power increases due to wind, waves, fouling and aging effects remain almost the same. The data shown in Figs. 9.1 and 9.2 support the credibility of this explanation.

Bigger power margins mean that the engine and propeller must be designed to keep high efficiency and reliability over a wider operation range. However, this is very difficult.

9.1 Definition of Powering Margin

The terms powering margin and sea margin are similar and are used in the community of ship designer, builder and operator. However, this term should be defined strictly.

Powering margin (sea margin) can be defined as the margin, by adding which at the estimation of the speed-power relationship for a newly built ship in calm water, the operation of the ship in realistic conditions can be obtained. In practice, this does not mean that a ship must meet full speed in all weather conditions, but can sustain its design speed over a realistic percentage of conditions such as 80-95% of the time.

It must have a strong correlation to the difference between the estimated speed and power relationship for a newly built ship in calm water and the expected speed and power relationship in real operating conditions after a certain period of operation. The components of the difference could be divided into the following:

▪ Powering margin to cope with the effects of environmental conditions.
▪ Powering margin to cope with the fouling and aging effects of hull & propeller surface and main engine.

9.2 Estimation of Powering Margin

"Estimation of powering margin for a ship" is, in reality, the "Estimation of required power at the supposed (extreme) operation condition which could be expected during the lifetime of the ship". In comparison with the result of power estimation for the newly built condition, we can obtain power margin. The simplified flow chart is shown in Fig. 9.3.

The procedure would consist of the following 4 stages:

(1) Propose the operating condition (Ship's displacement etc., sea state, relative wind speed, relative direction of waves and wind, ship's age etc.) where the powering margin is to be defined.
(2) Estimate resistance (including the increase due to the effects of environmental conditions) of the ship at the specified condition.
(3) Estimate hull, propeller and engine characteristics for the age of operation.
(4) Calculate speed and power relationship according to the ITTC Recommended Procedure on Predicting Powering Margins.

In the following, the explanations are made for (2) and (3) in the list above.

9.3 Estimation of Resistance Increase Due to the Effects of Environmental Conditions

For the estimation of resistance increase due to environmental effects, the ISO standard 15016 "Guidelines for the assessment of speed and power performance by analysis of speed trial data" gives quite comprehensive information, specifically in Annex A to Annex F of the standard. The content is also summarized in ITTC Recommended Procedure Analysis of Speed/Trial Data.

The components are as shown below:

1. Resistance increase due to wind.
2. Resistance increase due to waves.
3. Resistance increase due to steering.
4. Effect of restricted water.
5. Effect of water temperature and salt content.

9.4 Estimation of Resistance Increase Due to the Effects of Aging and Fouling of Hull & Propeller Surface

It was long been acknowledged that the resistance and powering characteristics of a ship are closely related to hull smoothness and

are adversely affected by ship fouling (Lowery, 1980). Investigation of ship fouling shows that ship resistance in still water can increase nearly 30 per cent one year after the last docking, and 50 per cent two years after the last docking. To maintain the initial speed two years after the last docking the power of a ship had to be increased from 50 to over 80 percent (Journée

and Meijers, 1980). While for ship propeller fouling, the required power may decrease by 20% (Mossad, 1986). The effect of the propeller surface condition is significantly important in terms of energy loss per unit area (Mossad, 1986). Such increases are now reduced due to improved hull surface treatments.
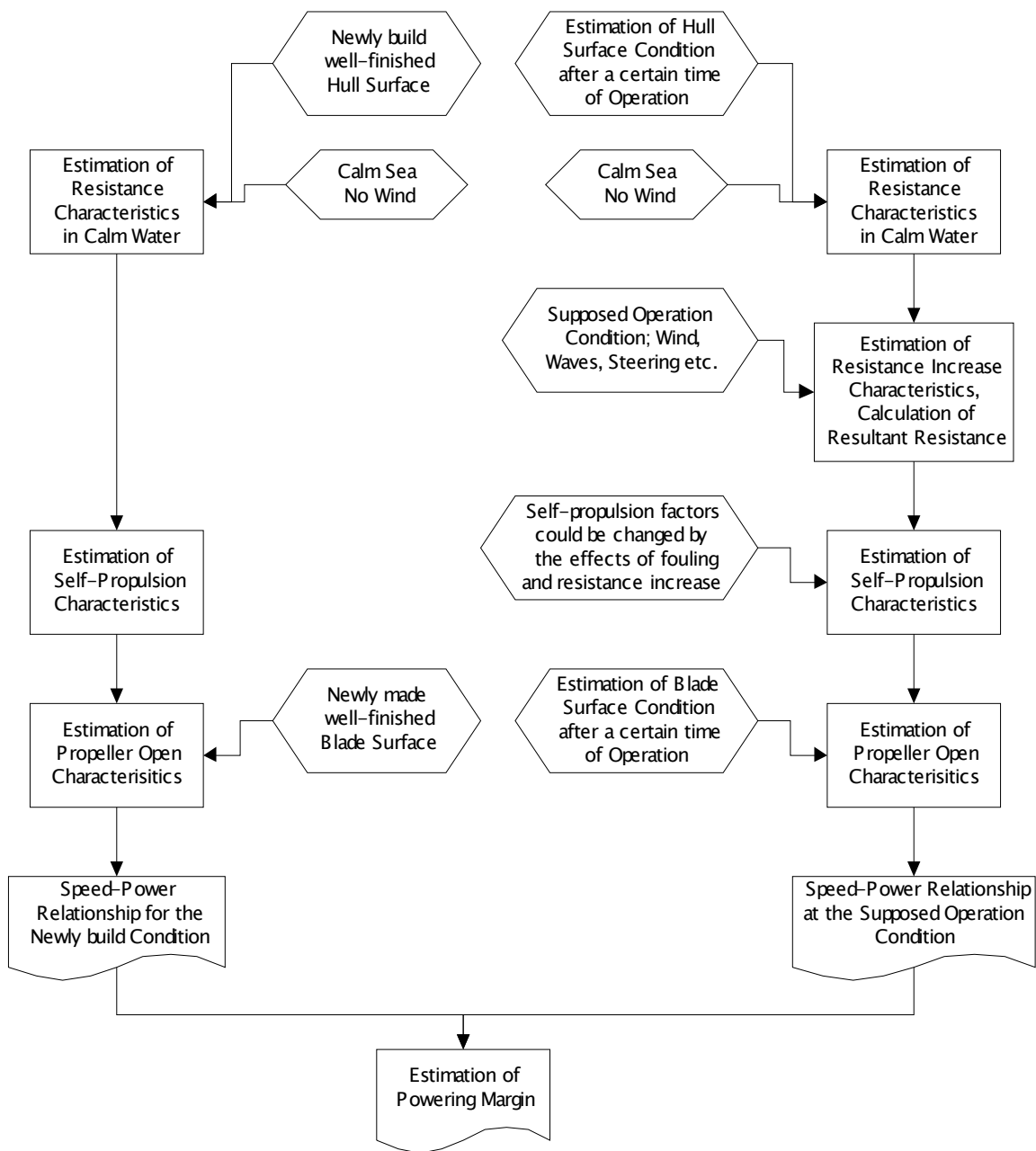

Figure 9.3- Simplified Flow Chart for the Estimation of Powering Margin.

As fouling is a biological phenomenon whose occurrence is difficult to predict and control (Townsin, 2003), there are many factors that influence a ship's degree of fouling. Among them, average voyage speed, types and age of antifouling paints, and average voyage duration were found to be highly significant accounting for 60% of variation in the available data. Of the three factors the most influential was the types and age of antifouling paints.

By far the biggest causes of propeller surface roughness is fouling, while a small roughness increase of a propeller causes large increase in the delivered power. In addition, propeller fouling can increase cavitation and noise radiation greatly (Lowery, 1980).

The international marine coatings **Hull Roughness Penalty Calculator** (a software to calculate hull roughness penalty) estimates the increase in power required over time for the four main antifouling technologies based on their average increase in physical hull roughness per year (Townsin, 2003, Townsin 2000, O'Leary and Anderson, 2003).

The combined effects of physical roughness and the risk of fouling on ship power required to maintain ship speed is shown in Figs. 9.4 and 9.5 (O'Leary and Anderson, 2003).
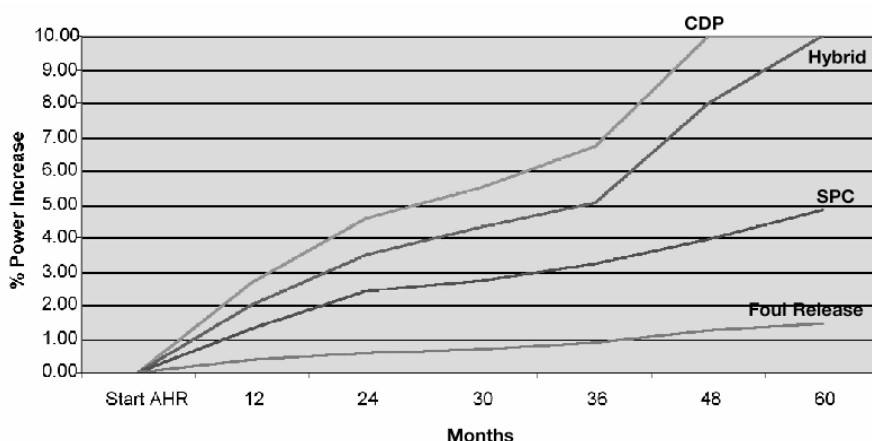

Figure 9.4- Overall % power increase for a typical fast fine ship (e.g. Container Liner) vs time for different antifouling types-Vertical sides.
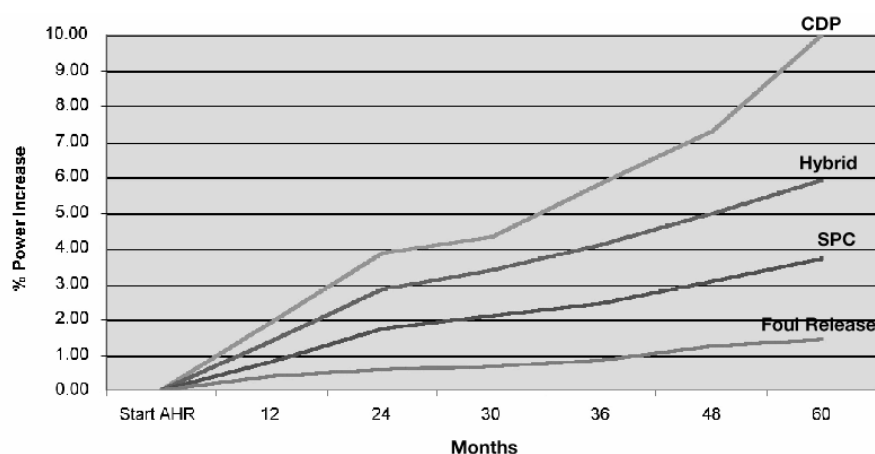

Figure 9.5- Overall % power/fuel increase for a typical fast fine ship (e.g. Container Liner) vs time for different antifouling types-Flat bottom.

It has been shown that antifouling paints play a decisive role in reducing ship fouling. Up to now, there is no an accurate and overall method to predict ship fouling. Only by studying a large number of ships over extended time periods can statistically reliable information be obtained. Utilizing different antifouling types is the mature measure, and further developing new and highly effective, non-contaminating antifouling types is a most effective step to reduce the ship fouling effect.

9.5 The Effects of Hull Roughness

The hull roughness or hull surface texture of a ship has a comparatively significant effect on the powering performance. It is considered that the hull roughness increases the frictional component of the ship resistance since it changes the boundary layer characteristics over the hull surface.

The hull roughness arises from a number of different causes. The types and causes of roughness can be summarized briefly as follows (Carlton 1994 and Byrne 1979):

1. Structural roughness
▪ - Plate waviness, weld seams, the condition of the steel surface, and so on.

2. Paint roughness
▪ Poor application of paint - Paint system failure such as blistering, detachment, and corrosion/pitting
▪ Build-up of old coatings such as the exhausted anti-fouling layer which is a honeycombed, powdery structure that accelerates paint system failure
▪ Mechanical damage such as berthing damage, damage from vessels coming alongside, cable chafe at the fore end, and so on.

3. Fouling roughness
▪ Undesirable growth of marine organisms on the hull surface

It is found that the local surface topography of relatively small scale has the greatest influence on the resistance. The standard measure of the hull roughness that has been adopted till now within the shipbuilding industry is Rt(50). This is a measure of the maximum peak to valley height or apparent amplitude over 50mm lengths of the hull surface. When undertaking a hull roughness survey with a hull roughness analyzer as proposed by BSRA (British Ship Research Association), the values of Rt(50) from 80~150 measured roughness profiles, each divided into 12 or 13x50 mm sampling lengths, will be determined. MHR (Mean Hull Roughness) is the mean of these Rt(50) values. According to Townsin et al. (1981), MHR can be statistically considered as AHR (Average Hull Roughness) if a full hull roughness survey is made.

However, there have been many arguments that the use of a simple parameter such as Rt(50) in representing random roughness is likely to be inadequate as surfaces having quite different roughness profiles can be numerically equal with respect to one parameter and yet be unequal with respect to others. So, extensive fundamental investigations to correlate the hull roughness with the resistance increment, e.g., the development of replica-based criteria (Musker and Lewkovicz, 1978, Johansson, 1985, and Walderhaug, 1986) have been made. Replica cards were reproduced in comparison with the surface of the actual ships and tested in a flow channel to determine their drag. When a particular replica card has been chosen as being representative of a particular hull surface, a power penalty is obtained from the correlation between measured roughness function and several statistical roughness parameters. For example, in the case of Musker's research (Musker and Lewkovicz, 1978), equivalent height obtained from a combination of statistical parameters such as the standard deviation, the average slope, the skewness and Kurtosis of the roughness height distribution instead of Rt(50) have been used to improve the correlation.

From the economic and practical viewpoint, the number and complexity of measured roughness parameters is limited. Townsin (1987) concluded that for rough surfaces in excess of around 250μm AHR, including surface damaged and deteriorated antifouling paint it is an unreliable parameter to correlate with resistance increase. However, Townsin and Dey (1990) demonstrated that Rt(50) can provide a reasonable estimate of the resistance increase for newly painted and moderately rough ship hulls less than 225μm AHR since it appears to correlate well with other available measures of roughness function. According to Townsin et al. (1986), it is found that the typical values of hull roughness for new ships have decreased over the decades and is of the order of 90~125μm. The hull roughness increases on average 20 μm /year for a surface coated with TBT-SPCs during the first ten years in service.

Lackenby (1962) proposed an early approximation from the analysis of hull roughness survey results and trial results made by BSRA that an increase in average roughness of 25μm would increase the resistance of a large, new single-screw ship by about 2.5%.

The Bowden-Davison formula proposed in 1974 was adopted at the 15th ITTC as the expression of correlation allowance intended for use when extrapolating ship resistance using the 1978 ITTC performance prediction method (Bowden and Davison, 1974, and ITTC, 1978):

$$C_A \times 10^3 = 105 \cdot \left(\frac{k_S}{L}\right)^{1/3} - 0.64$$

where k_S is the mean apparent amplitude of the surface roughness over a 50mm cut-off length, namely MHR and L is the ship length that should not exceed 400m. This formula was established from an analysis of thrust measurements taken during trials of 10 single screw ships. The roughness amplitudes actually measured for the ships were used when deriving the equation but it assumes a standard roughness of 150μm since actually measured roughness values are not always available. The

Bowden-Davison formula is not an accurate hull roughness penalty predictor since it can be regarded as one including not only the effects of roughness, but also all residual components in resistance predictions. Therefore, it should be recognized to be a correlation allowance including effects of roughness rather than a mere roughness allowance and it should not be used to predict the resistance increase due to a change in hull roughness.

Townsin et al. (1984) proposed a formula to use as a roughness penalty predictor instead of the Bowden-Davison formula in 1984 as follows:

$$\Delta C_f \times 10^3 = 44 \cdot \left[\left(\frac{AHR}{L}\right)^{1/3} - 10 \cdot R_n^{-1/3}\right] + 0.125$$

The Powering Performance Committee of the 19th ITTC (1990) suggested that where roughness measurements are available, the Bowden-Davison formula should be replaced by the above Townsin's formula and the difference between the ITTC correlation allowance obtained from the Bowden-Davison formula and the resistance increment by the hull roughness allowance obtained from Townsin's formula should be considered as a component caused by other phenomena not accounted for elsewhere:

$$\left(C_A - \Delta C_F\right) \times 10^3 = 5.86 - 0.6 \cdot \log R_n$$

The above equation implicitly predicates a small change in the slope of the ITTC extrapolator.

Recently, it has been found that the problem of fouling is much less important thanks to the great efficiency of modern antifouling paint such as TBT-SPC systems. However, alternatives to TBT-SPCs in preparation for the impending TBT ban of the IMO (2001) have been examined recently. Candries (2001) compared the drag, boundary layer and roughness characteristics of the surfaces coated with new antifouling paint systems such as Tin-free SPC

and Foul Release system, which are considered as currently the most satisfactory alternatives. In this research, roughness measurements of the tested surfaces have been carried out both with the BSRA Hull Roughness Analyzer as a stylus instrument and with a non-contacting optical measurement system and it is shown that for 2.5mm short cut-off lengths both the amplitude and texture parameters of the Foul Release system are significantly different from the Tin-free SPC coating. This means that other texture parameters will have to be included in the roughness analysis if the added drag of the surface coated with new paint systems such as the Foul Release is to be predicted accurately.

A draft procedure was prepared covering the prediction of powering margins.

10. CONCLUSIONS AND RECOMMENDATIONS

The survey to date conducted by the Committee indicates that there is no ITTC Member organization using RANS for commercial model-ship powering extrapolations.

Use of Monte Carlo methods have been evaluated by examining uncertainty in model scale total resistance and uncertainty in form factor determination. The Monte Carlo method was found to be more practical when there are correlated systematic errors and when data reduction equations are complex.

Uncertainty in extrapolation methods was assessed using a Monte Carlo technique and arbitrary levels of input uncertainty in the test parameters. Overall uncertainty in powering prediction was found to be less for an extrapolation based only on load varied self-propulsion tests than for the ITTC 1978 extrapolation method. However, this conclusion is tentative as the Committee had access to only one data-set where extensive load varied self-propulsion tests were done.

Existing methods to predict powering margins for high sea conditions, fouling and roughness need validation. The data needed to make these estimates is often not available during a sea trial.

An extensive data set of model tests and corresponding trials results has been collected for over 120 ships of varied type. Further, for a subset of these ships, model tests were done to extend the available data to include information for uncertainty analysis and load varied self propulsion tests.

To assess total accuracy in the power estimation procedure, about 1,200 sets of sea-trial data accumulated at one organization over more than 30 years were analyzed by using four different friction lines. The following results were obtained.

- From regression of the model-ship correlation factors obtained, standard deviations of estimated power and propeller revolutions were found to be around 5% and 1.5% respectively. These results were found to be almost independent of which friction line was used in the analysis.
- Mean values of the correlation allowance, C_A, were found to be close to zero. This means that the Reynolds number dependent part of ΔC_f can be expressed well by Townsin's formula since this method to estimate roughness was used in the analysis. However, the correlation coefficients depend not only on the friction line used, but also on the estimation procedure for full-scale propeller open characteristics and this organization uses a different procedure from that of the ITTC 1978 method (see Organization E in the table in Section 5.2).
- Validity of the roughness dependent part of Townsin's formula could not be verified, because the majority of the data was not accompanied by the results of hull roughness measurements.

10.1 Recommendations

- Adopt the Procedure: 7.5-04-01-01.1 Preparation and Conduct of Speed/Power Trials
- Adopt the Procedure: 7.5-04-01-01.2 Analysis of Speed/Power Trial Data
- Adopt the Procedure: 7.5-02-03-01.5 Predicting Powering Margins

11. REFERENCES

Bose, N. (Chairman), 1999, "Specialist Committee on Unconventional Propulsors: Final Report and Recommendations to the 22nd ITTC", 22nd ITTC, Vol. 2, 35 pages.

Bose, N. and Molloy, S., 2001, "Powering Prediction for Ships with Compound Propulsors", International Conference on Ocean Engineering, IIT Madras.

Bowden, B.S. and Davison, N.J., 1974, "Resistance Increments Due to Hull Roughness Associated with Form Factor Extrapolation Methods", NPL Ship TM 3800.

Byrne D., 1979, "Hull Roughness of Ships in Service", Trans. NECIES.

Candries, M., 2001, "Drag, Boundary-Layer and Roughness Characteristics of Marine Surfaces Coated with Antifoulings", Ph.D. Thesis, Dept. of Marine Technology, University of Newcastle upon Tyne.

Carlton J.S., 1994, "Marine Propellers and Propulsion", Butterworth-Heinemann Ltd.

Coleman, H.W. and Steele W.G., 1999, "Experimentation and Uncertainty Analysis for Engineers", 2nd Edition, John Wiley & Sons Inc, New York

Coutts, A.D.M., Haddon, M. and Hewitt, C.L., 1999, "Factors Influencing a Vessel's Degree of Fouling", 10th International Congress on Marine Corrosion and Fouling.

Holtrop, J., 2001, "Extrapolation of Propulsion Tests for Ships with Appendages and Complex Propulsors", Marine Technology, SNAME, New Jersey, USA, Vol. 38, No. 3, July.

Holtrop, J. and Hooijmans, P., 2002, "Quasi-steady model experiments on hybrid propulsion arrangements", Discussion to the 23rd ITTC, Venice.

Insel, M., Gustafsson, L. and Wiggins, A.D., 2005, Uncertainty in Form Factor Determination submitted for review for publication.

IMO, 2001, "IMO Adopts Convention on Control of Harmful Anti-fouling Systems on Ships", http://www.imo.org.

Ishii, N., 1975 "Actual Performance of Ships at Sea", Symposium on Propulsive Performance of Full Ships.

ITTC, 2002a, "Uncertainty Analysis, Example for Resistance Tests", 23rd ITTC, Venice, Quality Manual, Procedure 7.5-02-02-02 Rev 01.

ITTC, 2002b, "Final Report and Recommendation to the 23rd ITTC of the Specialist Committee on Speed and Powering Trials", 23rd ITTC, Vol. II, pp. 341-367, Venice, Italy.

ITTC, 1990, "Report of the Powering Performance Committee", 19th ITTC, Madrid, Spain.

ITTC, 1978, "Report of Performance Committee", 15th ITTC, Hague.

Johansson, L.E., 1985, "The Local Effect of Hull Roughness on Skin Friction. Calculations based on Floating Element Data and Three Dimensional Boundary Layer Theory", Trans. RINA, Vol. 127.

Journée, J.M.J. and Meijers, J.H.C., 1980, "Ship Routeing for Optimum Perform-

ance", Conference on Operation of Ships in Rough Weather, Transactions IME.

Katsui, T., Himeno, Y. and Tahara, Y., 2003, "Verification of Flat-Plate Friction Coefficient at Ship-Scale Reynolds Number", Proc. of International Symposium on Naval Architecture and Ocean Engineering, Shanghai, China.

Kracht, A., 1991, "Load Variation Tests Improve the Reliability of Ship Power Prediction Based on Model Test Results", Ship Technology Research Schiffstechnik, Schiffahrts-Verlag, HANSA, Hamburg, Germany, Vol. 38, No. 4, pp. 181-191.

Lackenby, H., 1962, "The Resistance of Ships with Special Reference to Skin Friction and Hull Surface Conditions", Trans. the Institution of Mechanical Engineers, London, England.

Lowery, L.H., 1980, "The Effects of Fouling Characteristics of U.S. Navy Surface Combatants", ITTC 80 (Proc. of the 19th General Meeting).

Matsubara, T., 1995, "Consideration as to Planned and Actual Performance of the Latest Commercial Vessels", 6th JSPC Symposium on Propulsive Performance of Ships at Sea.

Matsumoto, K., 2003, "Ship Design based on their Performance at Sea", 4th JTTC Symposium on Ship Performance at Sea.

Molloy, S., 2001, "Ship Powering Prediction Using Load Varying Self-Propulsion Tests", Masters degree thesis, Faculty of Engineering and Applied Science, Memorial University of Newfoundland.

Molloy, S. and Bose, N., 2001, "Ship Powering Prediction From Self-Propulsion Load Varying Tests", Proc. of the SP2001 Lavrentiev Lectures, St. Petersburg State Marine Technical University, St. Petersburg, Russia.

Molloy, S., 2005, Ph.D. thesis, Memorial University, in preparation.

Molloy, S., Bose, N. and Reilly, D., 2005, "Uncertainty in the ITTC 1978 power extrapolation method", Submitted for review.

Musker, A.J. and Lewkovicz, A.K., 1978, "The Effect of Ship Hull Roughness on the Development of Turbulent Boundary Layers", Proc. of the International Symposium on Ship Viscous Resistance, SSPA, Sweden.

Mossad, M., 1986, "Marine Propeller Roughness Penalties", Ph.D. Thesis University of Newcastle upon Tyne.

O'Leary, C. and Anderson, C.D., 2003, "A New Hull Roughness Penalty Calculator", International Marine Coatings.

Schmiechen, M., 1991, Proc. of the 2nd International Workshop on the Rational Theory of Ship Hull Propeller Interaction and its Applications, VWS, Berlin Ship Model Basin, HEFT 56.

Takahashi T. and Asai S., 1985, "Study on Rough-Sea Performance of Lower-Powered Large Full Ships", SNAME STAR Symposium.

Townsin, R.L., 2003, "The Ship Hull Fouling Penalty", International Marine Coatings.

Townsin, R.L., 2000, "Calculating the Cost of Marine Surface Roughness on Ship Performance", International Marine Coatings.

Townsin, R.L., 1987, "Developments in the Calculation of Rough Underwater Surface Power Penalties", 25th Anniversary Symposium, CETENA, Genoa, Italy.

Townsin, R.L., Byrne, D., Svensen, T.E. and Milne, A., 1986, "Fuel Economy due to Improvements in Ship Hull Roughness 1976-1986", International Shipbuilding Progress, Vol. 33.

Townsin, R.L., Byrne, D., Svensen, T.E., and Milne A., 1981, "Estimating the Technical and Economic Penalties of Hull and Propeller Roughness", Trans. SNAME.

Townsin, R.L. and Dey, S.K., 1990, "The Correlation of Roughness Drag with Surface Characteristics", Marine Roughness and Drag Workshop, London.

Townsin, R.L., Medhurst, J.S., Hamlin, N.A. and Sedat, B.S., 1984, "Progress in Calculating the Resistance of Ships with Homogeneous or Distributed Roughness", NECIES Centenary Conference on Marine Propulsion.

Walderhaug, H., 1986, "Paint Roughness Effects on Skin Friction", International Shipbuilding Progress, Vol. 33, No. 382.